

EFFECT OF TEMPERATURE ON MIXED-BED ION EXCHANGE
BASED ON LIQUID RESISTANCE CONTROLLED
REACTIVE EXCHANGE MODEL AT LOW
SOLUTION CONCENTRATIONS

By

SUHAS VASANT DIVEKAR

Bachelor of Chemical Engineering

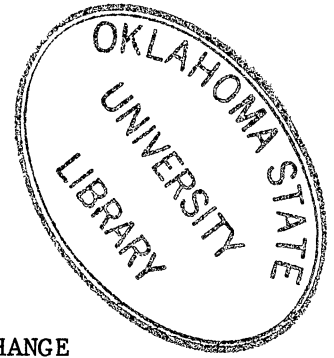
University of Bombay

Bombay, India

1984

Submitted to the Faculty of the
Graduate College of the
Oklahoma State University
in partial fulfillment of
the requirements for
the Degree of
MASTER OF SCIENCE
May, 1986

Thesis
1986
D618e
cap.2



EFFECT OF TEMPERATURE ON MIXED-BED ION EXCHANGE
BASED ON LIQUID RESISTANCE CONTROLLED
REACTIVE EXCHANGE MODEL AT LOW
SOLUTION CONCENTRATIONS

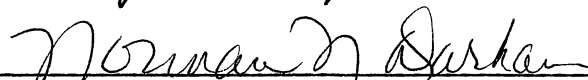
Thesis Approved:



Thesis Adviser







Dean of the Graduate College

PREFACE

This work involved the introduction of temperature effects in the current mixed-bed ion-exchange model. The aim was to obtain a more generalized model to predict mixed-bed ion-exchange phenomena at low concentrations.

I would like to express my heartfelt gratitude and appreciation to my adviser, Dr. Gary L. Foutch, for his guidance, helpfulness and friendliness throughout this study. Grateful acknowledgement is also extended to Dr. Mayis Seapan and Dr. Archibald G. Hill for serving on the advisory committee.

I wish to express my sincere thanks to Dr. Billy L. Crynes and Dr. Gary L. Foutch for the research and teaching assistantships which enabled me to pursue this study.

Special thanks are due to Chein-Tai Chen, Frank Hu, and Eugene Haub for their technical and moral support. I am very grateful to Kendra Thorp for her assistance in preparing this manuscript.

TABLE OF CONTENTS

Chapter	Page
I. INTRODUCTION	1
II. LITERATURE REVIEW.	4
Fundamentals of Ion Exchange.	4
Elementary Principles.	4
Structure and Properties of Ion Exchangers . .	6
Capacity	8
Equilibria.	8
Ion-Exchange Isotherm.	9
Separation Factor.	10
Selectivity Coefficient.	10
Distribution Coefficient	11
Thermodynamic Equilibrium Constant	12
Exchange as Competitive Sorption	13
Ion-Exchange as a Simple Donnan Equilibrium. .	14
Swelling Energy Theory	17
Complete Donnan Theory	18
Other Factors Affecting Selectivity.	21
The Effect of Temperature on Equilibria. . . .	22
Swelling	22
Swelling Pressure and Solvent Activity	23
Kinetics of Ion Exchange.	25
Particle Diffusion Control	27
Film Diffusion Control	29
Ion Exchange Accompanied by Reaction	32
Model for Mixed Bed Ion Exchange.	33
Temperature Dependent Terms in the Model.	34
Resin Selectivity Coefficients	34
Evaluation of Terms in Equation for Selectivity.	37
III. INTRODUCING TEMPERATURE EFFECTS.	41
Effect of Temperature on the Selectivity Coefficient	41
Correlating Temperature to Selectivity	43
Gregor's Model	43
Method of Kraus and Raridon.	43
Factors Affecting Resin Behavior	47

Chapter	Page
Effect of Temperature on Ionic Diffusion Coefficients	49
Effect of Temperature on Ionization Constant of Water	52
Effect of Temperature on Viscosity of the Bulk Solution Phase	53
IV. RESULTS AND DISCUSSION	56
V. CONCLUSIONS AND RECOMMENDATIONS	75
Conclusions	75
Temperature Dependent Parameters	75
Recommendations	77
BIBLIOGRAPHY	80

LIST OF TABLES

Table	Page
I. Variation of Selectivity Coefficient with Temperature on 16% DVB DOWEX-50 Resin (4)	42
II. Comparison of Calculated and Observed Values for Cupric-Hydrogen Exchange on 16% DOWEX-50 Resin (5).	42
III. Selectivity Coefficients for the Exchange of Tetramethylammonium with Sodium Ion for Various Equivalent Fractions (X_{TMA}) of 2, 4, 8% DVB Cross-linked Polystyrene Sulphonate	44
IV. Selectivity Coefficients for Various Compositions and Degrees of Crosslinking in the Sodium-Lithium Ion Exchange System (52).	45
V. Parameters in Kraus and Raridon Equation (41)	46
VI. Comparison of Observed and Calculated Values of the Selectivity Coefficients as a Function of Temperature Based on the Method of Kraus-Raridon (42).	47
VII. Variation of Equivalent Conductance with Temperature at Infinite Dilution.	51
VIII. Polar Liquid Viscosities.	54

LIST OF FIGURES

Figure	Page
1. Resin as an Osmotic Donnan System; Analogy Between Swollen Gel (b) and Colloidal Solution Under Osmotic Pressure (a)	15
2. Effect of Crosslinking and Degree of Exchange (X_k) on Selectivity.	17
3. Comparison of Osmotic Properties of Some Resins for Some Common Solutions.	19
4. Water-Vapor Sorption Isotherms of Ion-Exchange Resins. . .	24
5. Typical Binary Ion Exchange System (28)	27
6. Gregor's Model of the Ion Exchanger (28)	35
7. Temperature Dependence of Cation-Exchange Equilibria (Metal Tracers on DOWEX-50 Resin, H^+ Form)	44
8. Variation of Ionization Constant of Water with Temperature.	57
9. Variation of Ionic Diffusion Coefficients with Temperature.	58
10. Variation of Cationic and Anionic Selectivity Coefficients with Temperature	59
11. Variation of Solution Viscosity with Temperature	60
12. Variation of Sodium and Chloride Concentration Profiles with Temperature after 6 min. and Cation/Anion Ratio = 1.5.	61
13. Variation of Sodium Concentration Profiles with Temperature after 57 min. and Cation/Anion Ratio=1.5.	62
14. Variation of Chloride Concentration Profiles with Temperature after 57 min. and for Cation/Anion Ratio of 1.5	63

Figure	Page
15. Variation of Sodium Concentration Profiles with Temperature After 97 min. and for Cation/Anion Ratio of 1.5	64
16. Variation of Chloride Concentration Profiles with Temperature After 97 min. and for Cation/Anion Ratio of 1.5	65
17. Concentration Profiles for Mixed-Bed Ion Exchange with Neutralization in the Bulk Phase.	66
18. Concentration Profiles for Anion Exchanger with Neutralization in the Liquid Film.	66
19. Sodium Breakthrough Curves for Mixed-Bed Simulations with Temperature for Cation/Anion Ratio of 1.5	68
20. Chloride Breakthrough Curves for Mixed-Bed Simulations with Temperature for Cation/Anion Ratio of 1.5	69
21. Variation of Exchange Rate with Bulk Phase Concentration and Progress of Ion-Exchange (Film Reaction Model) . . .	71
22. Variation of Exchange Rate with Bulk Phase Concentration and Progress of Ion-Exchange (Film Reaction Model) . . .	72
23. Variation of R_i with Bulk Phase Concentration and Progress of Ion-Exchange for $C_{Cl}^0 = 1 \times 10^{-6} M$ (Film Reaction Model)	74
24. Experimental Set-Up for Mixed-Bed Ion-Exchange Studies . .	78
25. Jacketed Ion-Exchange Column (39).	79

NOMENCLATURE

a_i	activity of ionic species i
a_s	specific surface area, $\text{cm}^2 \text{ area}/\text{cm}^3 \text{ resin}$
\bar{C}	total concentration of fixed ionic groups in resin, meq/cm^3
C_i	concentration of species i , meq/cm^3
C_t	total counterion concentration, meq/cm^3
d_p	particle diameter, cm
D	effective system diffusivity, cm^2/s
D_e	effective liquid phase diffusivity, cm^2/s
D_i	diffusion coefficient of species i , cm^2/s
e	fractional pore volume
f_c	volume cation resin/total resin volume
F	Faraday's constant, coulombs/mole
F_1	volumetric flow rate, cm^3/s
G	Gibb's Free Energy, cal/mole
h	reaction plane position
H	Heat of reaction cal/mole
J_i	ionic flux of species i , $\text{meq}/\text{s cm}^2$
k	second order rate constant, $\text{cm}^3/\text{meq s}$
k_1	nonionic liquid phase mass transfer coefficient, cm/s
k_1	ionic liquid phase mass transfer coefficient, cm/s
k_B^A	equilibrium constant
$N_{k_B^A}$	rational equilibrium constant

K_{A}^{B}	selectivity coefficient for ion B in the solution replacing ion A in the resin phase
K_w	dissociation constant of water
m_i	molality of species i
N_m^0	weight normality of the fully swollen exchanger
n	total number of exchanging species
P	pressure, atm
P_s	swelling pressure, atm
q_i	mean resin phase concentration of species i, meq/cm ³
Q	total resin exchange capacity, meq/cm ³
r	radial distance
r_o	particle radius, cm
R	universal gas constant
R_i	ratio of electrolyte to nonelectrolyte mass transfer coefficients
Sc	Schmidt number, dimensionless
Sh	Sherwood number, dimensionless
t	time, s
T	absolute temperature, K
\bar{V}_i	partial molar volume of ionic species i in the resin, cm ³
V	volume of solution having passed a given column layer, cm ³
V_a	equivalent volume of the dry exchanger, cm ³
V_f	volume of solution fed to column, cm ³
V_S	solution volume which is stoichiometrically equivalent to bed capacity
x_i	equivalent fraction of species i in solution
x_w	equivalent water content
\bar{X}	total ion concentration in resin phase per unit volume of bed, meq/cm ³

\bar{X}_i	concentration of species i in resin phase per unit volume of bed, meq/cm ³
y	distance normal to solid-liquid interface, cm
y_i	equivalent fraction of species i in resin phase
Z	distance from column inlet, cm
Z_i	ionic charge of species i

Greek Letters

α	ratio of exiting to entering ion diffusivities
$\alpha_{\frac{A}{B}}$	separation factor, Equation II-3
γ_i	activity coefficient of species i
δ	liquid film thickness, cm
ϵ	bed void fraction
μ	superficial liquid velocity, cm/s
λ	electrical conductance (Equation III-4)
μ_1	solution viscosity, cp
ϕ	electric potential, ergs/coulomb

Superscripts

bar	refers to resin phase
*	interfacial equilibrium condition
1	cation exchange parameter
2	anion exchange parameter
f	column feed condition
o	bulk phase condition
r	reaction path condition

Subscript

A	ion exiting the resin phase
B	ion entering the resin phase
c	chloride ion

h hydrogen ion
i species i
n sodium ion
o hydroxide ion
r at the reaction plane

CHAPTER I

INTRODUCTION

The development of a generalized model simulating the phenomenon of mixed-bed ion exchange is the objective of this work. Deionization by mixed-bed ion exchange serves as an economical and convenient method to produce high purity water. The mechanical power generation and semiconductor industries require large quantities of very pure water. The demand for pure water has pressured the water purification industry considerably in the recent years (11,71). An accurate and generalized mathematical model predicting the rates of mixed-bed ion exchange would be of great help. Mixed-bed deionization technology and industrial practice are well ahead of the corresponding theory of ion exchange accompanied by chemical reaction. The majority of the articles on mixed-bed ion exchange has been concerned with proper design, operation, and maintenance of these units instead of the ion exchange theory. Other articles deal with finding approximate correlations relating breakthrough time with fluid flow rates, inlet concentrations, resin capacities, etc.

This work is based on a previous mixed-bed ion-exchange model (25) generalized by introducing the effect of temperature on equilibria and the kinetics of ion exchange. The previous model was developed without considering the effect of temperature, with parameters assigned their respective values at 25°C. This modification of the

previous model has temperature as a variable. Thus, the effect of temperature on the kinetics and equilibria of mixed-bed ion exchange can be rigorously studied with this model.

At present, data on temperature effects is crude and scarce. Much of the work has studied the effect of temperature on the selectivity coefficient, based on rigorous thermodynamic fundamentals (20,21,24,37,38,46). Some researchers have circumvented the complexities and fundamental problems associated with the physical nature of the ion-exchange phenomenon by fitting experimental curves to laboratory data. Others have used the osmotic approach to ion-exchange equilibrium. However, no specific literature on temperature effects in mixed-ion exchange columns is readily available.

The work presented here consists of obtaining appropriate expressions for the temperature dependent terms in the selected model. The original model (25), was based on the desire to simulate certain column variables and exchange conditions which are not generally considered in current mixed-bed ion-exchange models. These include consideration of the following effects: variation of the cation-to-anion resin ratio; differing cation and anion exchange rates, exchange capacities, and particle sizes; reversibility of exchange at low concentrations; neutralization reactions within the film and bulk-liquid phases; and effluent ion concentrations on the order of one part per billion (1×10^{-7} M). All of the above considerations were included in the mixed-bed model by accounting for the position of the neutralization reaction front and the water dissociation constant in separate flux equations for the cation and anion resins. These flux equations were based on the Nernst-Planck theory in conjunction with

the static film model and nonionic mass transfer coefficient correlations for packed beds. The use of the static-film model allows part of the flux equations to be analytically integrated. The ion-flux equations used do not account for the exchange resistance due to particle diffusion within the exchange resins. Other inherent assumptions in the model are: uniform bulk liquid and surface compositions exist for a given exchange particle; equilibrium occurs at the particle-film interface; neutralization reactions are instantaneous compared to the rate of exchange; activity coefficients are unity for the concentrations studied; mass transfer is pseudo-steady state across the film layer; the system is isothermal (temperature between 15° and 80° C); and dispersion may be neglected in the mixed bed.

Thus, with the introduction of temperature as a variable, the resulting model is a more powerful and generalized tool for simulating the phenomenon of mixed-bed ion exchange in columns at ultra-low concentrations (0.001 meq/cc).

CHAPTER II

LITERATURE REVIEW

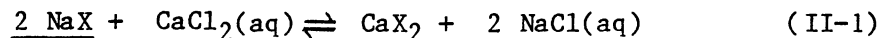
The topics presented here are: ion exchange fundamentals, mixed-bed ion-exchange modeling and effect of temperature on ion-exchange equilibria.

Fundamentals of Ion Exchange

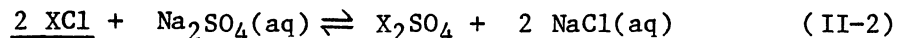
Elementary Principles

Ion exchangers are insoluble solid materials which carry exchangeable cations or anions. These ions can be exchanged for a stoichiometrically equivalent amount of other ions of the same charge when the ion exchanger is in contact with an electrolyte solution. Carriers of exchangeable cations are called cation exchangers, and carriers of exchangeable anions, anion exchangers (27).

A typical cation exchange is



and a typical anion exchange is



where, X represents a structural unit of the ion exchanger; solid phases are underlined; and aq indicates that the electrolyte is in aqueous solution.

Ion exchange is a reversible process, which resembles sorption, in that a dissolved species is taken up by a solid. However, unlike sorption, ion exchange is a stoichiometric process. Every ion removed from the solution is replaced by an equivalent amount of another ionic species of the same charge.

When an ion exchanger has lost all of its exchangeable ions, it is exhausted. The resin can now be restored to its original state by the reverse process, called regeneration. During regeneration, the ion exchanger is contacted with an aqueous solution containing the original ions possessed by the exchanger. Ion exchangers owe their characteristic properties to a unique feature of their structure. They consist of a framework held together by chemical bonds or lattice energy. This framework carries a positive or negative electric surplus charge which is compensated by ions of opposite sign, called counter-ions. The counter-ions are free to move within the framework and can be replaced by other ions of the same charge. The framework of a cation exchanger can be regarded as a macromolecular or crystalline polyanion, and that of an anion exchanger as a polycation. The inactive ions which do not take part in the ion exchange process are called co-ions. These are mobile ions with charges of the same sign as the framework charge. The counter-ion content of the ion exchanger thus depends not only on the magnitude of the framework charge but also on its co-ion content.

Mass transfer by diffusion plays the most important part in ion exchange. The migration of ions is hindered both by particle and film diffusion. Ion exchangers have an irregular, three dimensional framework which presents considerable resistance to ions diffusing into and

out of the exchanger framework. The film resistance is pronounced at low flow rates due to the presence of the stagnant film surrounding the exchanger particles, which are generally in the form of tiny spheres. The chemical factors are remarkably insignificant in ion exchange. Ion exchange is really a process accompanied by redistribution of ions and by diffusion rather than actual chemical reaction. The absence of an actual chemical reaction also explains why the heat evolved in the course of ion exchange processes is usually rather small (often less than 2 kcal/mole), unless the ion exchange is followed by reactions such as neutralization, etc.

Structure and Properties of Ion Exchangers

Many different natural and synthetic products show ion exchange properties. The most important of these are ion exchange resins, ion exchange coals, mineral ion exchanges, and synthetic inorganic ion exchangers. Several other types are known, but are either obsolete or used only for highly specialized purposes.

The general structural principle, a framework with electric surplus charge and mobile counter-ions is common to all ion exchangers. Nevertheless, the various types of materials show marked differences in behavior.

The most important class of ion exchangers are the ion exchange resins. Since the mixed-bed ion-exchange model under consideration uses this variety of ion exchangers, they are discussed in some detail here. Ion exchange resins are typical gels. Their framework consists of an irregular, macromolecular, three-dimensional network of hydrocarbon chains. The matrix carries ionic groups such as (27)



in cation exchangers, and



in anion exchangers. Ion-exchange resins thus are crosslinked polyelectrolytes. The matrix of the resin is hydrophobic. However, hydrophilic components are introduced by the incorporation of ionic groups such as $-\text{SO}_3^-\text{H}^+$. Linear hydrocarbon macromolecules with such groups are soluble in water. The ion-exchange resins, in contrast are made insoluble by introduction of crosslinks, which interconnect the various hydrocarbon chains. An ion exchange resin particle is practically one single macromolecule. Its dissolution would require rupture of carbon-carbon bonds. Thus, the resins are stable in all solvents by which they are not dissolved. However the matrix is elastic and can be expanded. Hence, the resins can swell by taking up solvent.

The chemical, thermal, and mechanical stability of the resins depend chiefly on the structure and degree of crosslinking of the matrix and on the nature and number of the fixed ionic groups. Resin deterioration can be caused by thermal and chemical means, eg. thermal hydrolysis and oxidation. Most resins are stable in all common solvents, except in the presence of strong oxidizing or reducing agents, and withstand temperatures up to slightly more than 100° C. Strong-base anion exchange resins begin to deteriorate above 60° C.

The ion exchange behavior of the resins is determined chiefly by the fixed ionic groups. The number of groups determines the ion

exchange capacity. The chemical nature of the groups greatly affects ion exchange equilibria. An important factor is the acid or base strength of the groups. The nature of the fixed groups also affects the selectivity of the resins. Counter-ions, which tend to associate with the fixed ionic groups by forming ion pairs or complexes, are preferred by the resin.

Innumerable types of ion exchange resins with different properties can be prepared. Not only the number and nature of the fixed ionic groups, but also the composition and the degree of crosslinking of the matrix can be varied and adapted to intended applications.

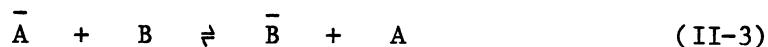
Capacity

Ion exchangers are characterized in a quantitative manner by their capacity which is defined as the number of counter-ion equivalents in a specified amount of material. The definition of capacity helps in characterizing ion exchangers and numerical calculations of ion exchange operations. Capacity is defined in several different ways for convenience. The weight capacity is expressed in milliequivalents per gram of the ion exchanger. The volume capacity is expressed in equivalents per liter of the fully swollen bed. Another important definition is the apparent capacity, which is a phenomenological quantity indicating how many counter-ions the ion exchanger can take up under specified conditions.

Equilibria

Ion-exchange equilibrium is attained when an ion exchanger is placed in an electrolyte solution containing a counter-ion which is

different from that in the ion exchanger. Suppose that the ion exchanger is initially in form A, and the counter-ion in the solution is B. Counter-ion exchange occurs, and the ion A in the ion exchanger is partially replaced by B:



In equilibrium, both the ion exchanger and the solution contain both competing counter-ion species, A and B (40).

The exchange (II-3) is reversible. The concentration ratio of the two competing counter-ion species in the ion exchanger is usually different from that in the solution; as a rule, the ion exchange selects one species in preference to the other. The degree of preference for one ionic species over the other is expressed in terms of the selectivity coefficient. Since the selectivity coefficient is an important function of temperature, and strongly affects ion exchange equilibrium, it is discussed in detail here.

Ion exchange equilibria are of great practical and theoretical importance. For convenience, the following definitions are commonly used.

Ion-Exchange Isotherm

The ion-exchange isotherm shows the ionic composition of the exchanger as a function of the experimental conditions. Various representations can be used. As a rule, the equivalent ionic fraction, \bar{x}_A , of the counter-ion A in the ion-exchanger is plotted as a function of the equivalent ionic fraction x_A in the solution while the other variables are kept constant. The equivalent ionic fraction is defined by

$$x_A = \frac{z_A m_A}{z_A m_A + z_B m_B} \quad (\text{II-4})$$

Separation Factor

The preference of the ion exchanger for one of the two counter-ions is often expressed by the separation factor. This quantity is particularly convenient for practical applications such as column operation. The separation factor, α_B^A , is defined by

$$\alpha_B^A = \frac{\bar{m}_A m_B}{\bar{m}_B m_A} = \frac{\bar{C}_A C_B}{\bar{C}_B C_A} = \frac{\bar{x}_A x_B}{\bar{x}_B x_A} \quad (\text{II-5})$$

The separation factor is the quotient of the concentration ratios of the two counter-ions in the ion exchanger and the solution. If the ion A is preferred, the factor α_B^A is larger than unity, and if B is preferred, the factor is smaller than unity. The numerical value of the separation factor is not affected by the choice of the concentration units. The separation factor is a function of the total concentration of the solution, the temperature, and the equivalent fraction x_A .

Selectivity Coefficient

The selectivity coefficient can be conveniently used to describe ion-exchange equilibria. This coefficient is more convenient for theoretical studies. The molal selectivity coefficient is defined by

$$K_B^A = \frac{\bar{m}_A^{z_B} \bar{m}_B^{z_A}}{\bar{m}_B^{z_A} \bar{m}_A^{z_B}} \quad (\text{II-6})$$

Molarities or equivalent ionic fractions may be used instead of molalities:

$$K'_{B^A} = \frac{\bar{C}_A^{z_B} C_B^{z_A}}{\bar{C}_B^{z_A} C_A^{z_B}} \quad N_{K_B^A} = \frac{\bar{x}_A^{z_B} x_B^{z_A}}{\bar{x}_B^{z_A} x_A^{z_B}} \quad (\text{II-7})$$

The quantities K'_{B^A} and $N_{K_B^A}$ are the molar and the rational selectivity coefficients, respectively.

The essential difference between the separation factor and the selectivity coefficient is that the latter contains the ionic valences as the exponents. Thus, the separation factor is usually different from the selectivity coefficient if the valences of the competing counter-ions are not equal. In such cases, the selectivity coefficient remains more nearly constant when the experimental conditions, particularly the total solution concentration, are varied.

Distribution Coefficient

In certain practical applications, equilibrium is most conveniently expressed in terms of the distribution coefficients of the counter-ions. The molal and molar distribution coefficients are defined by

$$\lambda_i = \frac{\bar{m}_i}{m_i} = \frac{\bar{x}_i \bar{m}}{x_i m} \quad (\text{II-8})$$

and

$$\lambda'_i = \frac{\bar{C}_i}{C_i} = \frac{\bar{x}_i \bar{C}}{x_i C} \quad (\text{II-9})$$

For any given conditions, the distribution coefficient can be calculated from the selectivity coefficient. However, there is no simple explicit relationship between these two quantities. The use of the distribution coefficient is particularly advantageous if the species is only a trace component (for example, $m_A \ll m$, $\bar{m}_A \ll \bar{m}$, and consequently $\bar{m}_B/m_B = \bar{m}/m$). In such cases, the exchange extends over only a short section of the isotherm near the origin. Usually, this short section is practically linear. For the range under consideration, the distribution coefficient is independent of x_A .

Thermodynamic Equilibrium Constant

This is used in theoretical studies. It is defined by the thermodynamic relation

$$\Delta G^{\circ} = - R T \ln k_B^A \quad (\text{II-10})$$

where, ΔG° is the standard free change of the ion exchange (II-3) and the sorption and desorption of solvent and electrolytes by which this process is necessarily accompanied, and where k_B^A is the equilibrium constant.

In contrast to the separation factor, the selectivity coefficient, and the distribution coefficient, which all refer to a given set of experimental conditions, and thus correspond to one specific point on the isotherm surface, the equilibrium constant is an integral quantity characteristic of the whole isotherm surface and is a true constant depending on the temperature only. Accordingly, the equilibrium constant gives no information about the exact counter-ion distribution under any particular experimental conditions.

A simple relation between the thermodynamic equilibrium constant and the activities of the counter-ions exists if the electrolyte sorption and changes in swelling can be neglected. In this case, the equilibrium constant is

$$k_B^A = \frac{a_A^{-z_B} a_B^{z_A}}{a_B^{-z_A} a_A^{z_B}} \quad (\text{II-11})$$

The relations (II-10) and (II-11) show that the numerical value of the equilibrium constant depends on the choice of standard states. Often, the molal scale is used for both the ion exchanger and the external solution. Here, the reference state (activity coefficients equal to unity) is a solution or a (fictitious) pore liquid of infinite dilution, and the standard state (activity equal to unity) is an approximately one molal solution or pore liquid (the deviation from 1 molar is given by the activity coefficient, which is defined by the choice of the reference state). The equilibrium constant obtained by this choice of reference states is called the molal equilibrium constant. Another way is to treat the ion exchanger as a solid solution of the swollen resins and both the standard and reference states of the two resins are taken to be the respective monoionic forms of the ion exchanger in equilibrium with water. The constant obtained in this way is called the rational equilibrium constant.

Exchange as Competitive Sorption

If a resin can be regarded as having a definite number of ionic sites, then selectivity can be treated as the simultaneous competition

of ions A^+ and B^+ (for cations) for the available sites. If the sites are independent of each other, the Langmuir adsorption theory would be applicable. This shows that the pressure, and therefore activity of a single adsorbate in equilibrium with the surface on which it covers a fraction, θ , of the available sites, is proportional to $\theta/(1-\theta)$, i.e. fraction covered/fraction vacant. For two adsorbates, A and B, covering fractions X_A and X_B of the available capacity of the resin,

$$\frac{\text{Activity of A}}{\text{Activity of B}} = \frac{\bar{C}_A \bar{\gamma}_A}{\bar{C}_B \bar{\gamma}_B} = \frac{k_A \bar{X}_A / (1 - \bar{X}_A - \bar{X}_B)}{k_B \bar{X}_B / (1 - \bar{X}_A - \bar{X}_B)} = \frac{k_A \bar{C}_A}{k_B \bar{C}_B} \quad (\text{II-12})$$

where k_A and k_B are constants for the two ions and depend on their heats of sorption. This model thus predicts that the selectivity coefficient is constant, equal to k_B/k_A , and independent of X_A . The sorption sites are thought to be independent of each other. The situation is not altered by the fact that the adsorbates, A and B, are ions which would be attracted to the ionic sites with different energies owing to their different sizes. Thus, the model depicts the ideal solution case. To extend this model to the non-ideal case would require information on the interaction between the adsorbate ions. This cannot be treated in a simple way using the adsorption theory (40).

Ion-Exchange as a simple Donnan Equilibrium

Bauman and Eichhorn (28) suggested that ion-exchange resins could be regarded as concentrated solid electrolyte solutions. This model is justified for resins that contain considerable amounts of water,

and but for the cross-links they would be liquid solutions of chain poly-electrolytes. The chains are flexible but the cross links prevent the chains from breaking apart and diffusing into the aqueous phase. It is reasonable to compare the resin phase with a colloidal poly-electrolyte solution contained in a semi-permeable bag which permits passage of solvent and small ions, but repels the colloidal ions (Figure 1).

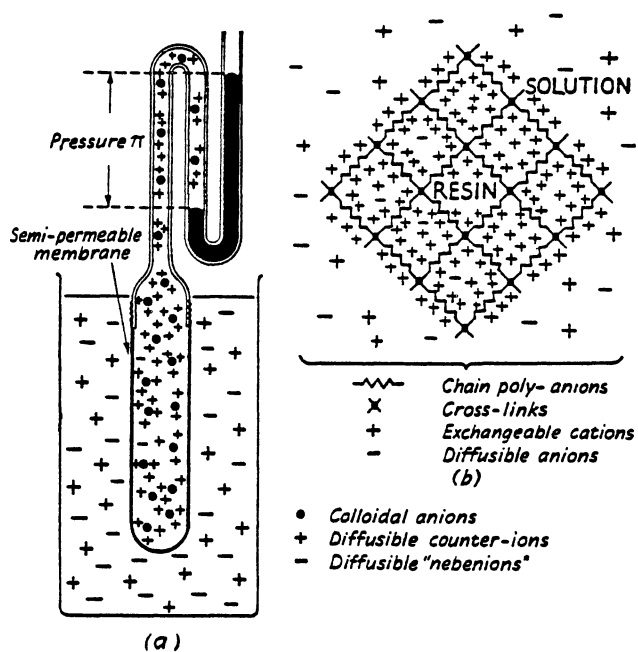


Figure 1. Resin as an Osmotic Donnan System; Analogy Between Swollen Gel (b) and Colloidal Solution Under Osmotic Pressure (a).

Such systems, in which one type of ion is imprisoned because of its large size while others distribute themselves freely between two

phases, are called Donnan systems, and the phenomenon is called the Donnan membrane equilibrium. At equilibrium, the ionic activity product of any permeable electrolyte is the same inside and outside the resin, e.g. for sodium chloride

$$(\bar{a}_{\text{Na}^+})(\bar{a}_{\text{Cl}^-}) = (a_{\text{Na}^+})(a_{\text{Cl}^-}) \quad (\text{II-13})$$

Hence, if a cation-exchange resin is in equilibrium with an aqueous solution containing A^+X^- and B^+X^- (X^- being a permanent anion), the Donnan equation applies to both of these electrolytes simultaneously, and hence

$$\frac{(\bar{a}_{\text{A}^+})(\bar{a}_{\text{X}^-})}{(\bar{a}_{\text{B}^+})(\bar{a}_{\text{X}^-})} = \frac{(a_{\text{A}^+})(a_{\text{X}^-})}{(a_{\text{B}^+})(a_{\text{X}^-})} \quad (\text{II-14})$$

The selectivity coefficient is then given by

$$K_{\text{A}}^{\text{B}} = \frac{\bar{C}_{\text{B}} C_{\text{A}}}{\bar{C}_{\text{A}} C_{\text{B}}} = \frac{\bar{\gamma}_{\text{A}} \gamma_{\text{B}}}{\bar{\gamma}_{\text{B}} \gamma_{\text{A}}} \quad (\text{II-15})$$

This theory indicates that selectivity arises from differences in the ratio of the activity coefficients of the two cations in the resin phase as compared with the ratio in the bulk solution phase. Support for this theory is provided by studies of the influence of charge density on selectivity. This is because specific interaction effects become more marked as the concentration is increased and selectivity should increase with internal ionic concentration. The predicted effect is seen with sulphonated polystyrene resins with different degrees of cross-linking. Those with low cross-linking show little selectivity compared with those with high cross-linking; the latter are less swollen and therefore more concentrated (Figure 2).

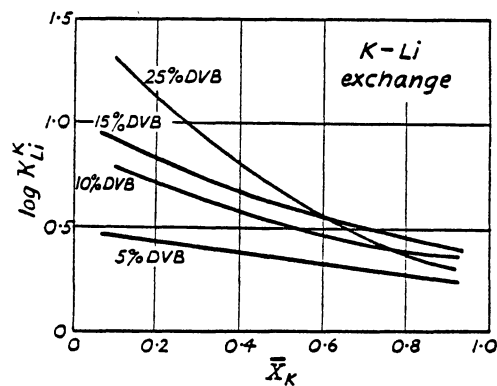


Figure 2. Effect of Crosslinking and Degree of Exchange (\bar{X}_K) on Selectivity

The conclusion of this theory is that inter-ionic forces inside the resin are a major factor in determining selectivity.

Swelling Energy Theory

In this theory, the elastic properties of the resin are considered. Normally, a concentrated salt solution cannot be in equilibrium with a dilute solution at the same pressure if the phase boundary is permeable to the solvent, as osmosis will take place; if the concentrated solution is contained in a semi-permeable membrane, its pressure will increase until the equilibrium osmotic pressure is reached. In the case of a resin, absorption of water causes the polymer network to stretch and set up an internal 'swelling pressure' (actually tension), P_s , which has the same thermodynamic effect as an externally applied osmotic pressure - it increases the chemical poten-

tial of any species, i , inside the resin by an amount $P_s \bar{V}_i$, where \bar{V}_i is the partial molar volume of i in the resin.

It follows that the chemical potentials of two ions, X and Y , will differ by $P_s(\bar{V}_X - \bar{V}_Y)$, and thus the resin will tend to show a preference for the smaller ion (other factors being equal). Gregor (20) was the first researcher to suggest that the selectivity coefficients might be accounted for on this basis alone. If chemical activity coefficient effects are negligible compared with the swelling energy, the selectivity coefficient is given by

$$R T \ln K_X^Y = P_s(\bar{V}_X - \bar{V}_Y) \quad (\text{II-16})$$

Complete Donnan Theory

This theory includes both an activity coefficient term (to allow for 'chemical' interaction of the ions) and a swelling energy term. The corresponding equation was given by Donnan as a particular case of his comprehensive thermodynamic theory of membrane equilibria. The selectivity coefficient is given by

$$\ln K = \ln (\gamma_B / \gamma_A) - \ln (\bar{\gamma}_B / \bar{\gamma}_A) + P_s (\bar{V}_A - \bar{V}_B) / (R T) \quad (\text{II-17})$$

This theory involves the plausible assumption that the mechanical and chemical work terms can be separated; that is, $\bar{\gamma}_A/\bar{\gamma}_B$ is considered dependent only on the chemical composition of the resin, and the mechanical term, $P_s(\bar{V}_A - \bar{V}_B)/R T$, dependent only on the stretching of the network, and therefore on the total swollen volume of the resin.

Although it is not possible to check equation (II-17) accurately by direct experiment, its approximate validity is indicated by the work of Glueckauf (17). The term $\ln \gamma_B/\gamma_A$ for the solution can be calculated by the extended Debye-Huckel theory since the external solution is generally dilute. The values can be determined by isopiestic vapor-pressure measurements on resins of very low degrees of crosslinking for which P_s is negligible, the assumption being made that $\bar{\gamma}$ is dependent only on the internal molality of the ions and independent of the cross-linking. This assumption is not accurate, but evidence supports the analogy between a swollen 'resinate' and an ordinary concentrated salt solution (Fig. 3).

The ratio of the activity coefficients of the two ions in the resin is calculated using the semi-empirical Harned rule. This rule is observed for certain pairs of salts in aqueous solution (27).

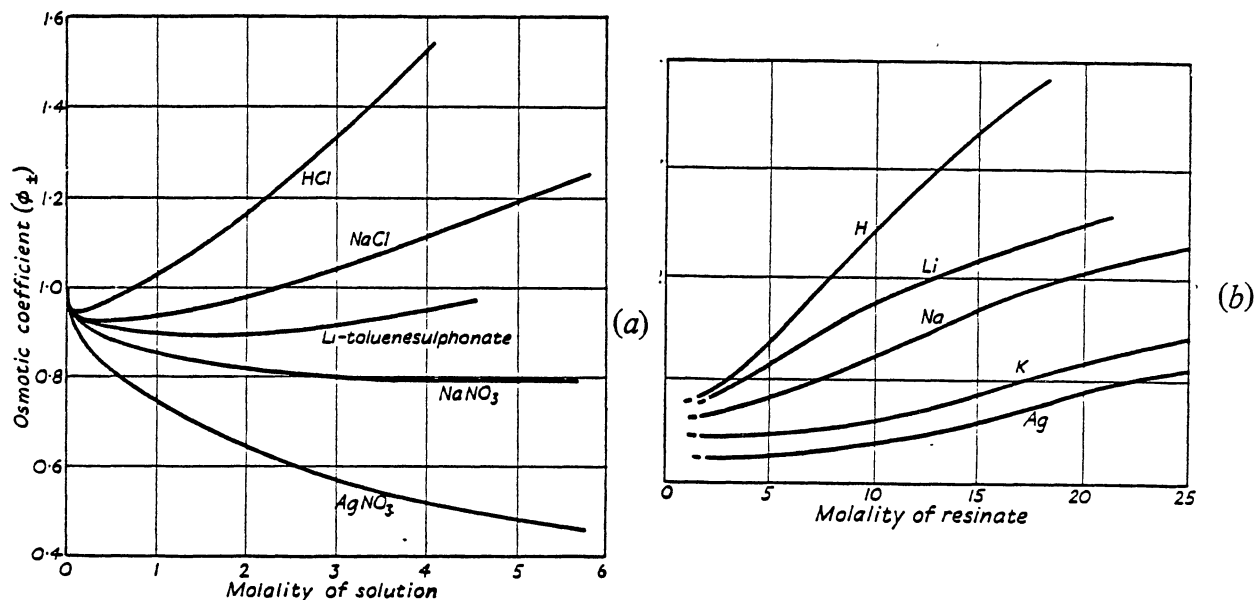


Figure 3. Comparison of Osmotic Properties of Some Resins for Some Common Solutions

However, the Harned rule is not widely applicable, and is known to be invalid for a mixture of p-toluenesulphonic acid and its sodium salt.

The swelling pressure can be calculated from water-vapor sorption isotherms determined by the isopiestic method with resins of the same salt but different degrees of cross-linking. The assumption is made that at equal water contents (per g equiv.) two resins of different cross-linking have the same chemical activity coefficients, but differ in water-vapor activity due to different swelling pressures. The free energy change on transferring a mole of water from a resin of low cross-linking ($P_s = 0$) to one of higher cross-linking (at the same molality) is then given by $G = R T \ln p_2/p_1$ (where p_1 and p_2 are the equilibrium vapor pressures over the two resins), this can be equated with the mechanical work involved in transferring water, of molar volume V_w (= 18 ml) from a phase of negligible pressure to one at pressure P_s . It follows that

$$P_s V_w = R T \ln p_2/p_1$$

After all these quantities have been determined, the final test is whether the right-hand side of Equation (II-17) predicts selectivity coefficients in agreement with experiment. In practice, only very rough agreement is obtained. The experimental finding is that K_A^B is not a true equilibrium constant, but changes considerably with changes in the proportion of A^+ to B^+ in the resin. This is qualitatively explained by the theory, but is not accurately represented.

Overall, Equation (II-17) does provide a sound representation of ion-exchange equilibria, but does not accurately predict selectivity coefficients. The chief difficulty is in assessing the important activity coefficient ratio $\bar{\gamma}_B/\bar{\gamma}_A$. The influence of swelling energy

is generally negligible except for highly cross-linked resins or large ions.

Other Factors Affecting Selectivity

The Sieve Effect. Large ions are prevented from entering the pores of the resin structure because of their size, and hence cannot partake in ion-exchange in that resin. The resin is expandible and can be thought of as "elastic sieves". The tension in the resin increases with the degree of crosslinking.

Sorption by van der Waals Forces. These forces are important when dealing with large ions. This is confirmed from the fact that the order of preference for ions can be opposite of that expected by steric composition and Coulombic attraction. Here, non-Coulombic van der Waals forces come into play and reverse the order of preference.

Change of Selectivity With Ion-Fraction, X , in the Resin. The selectivity coefficient K_A^B decreases markedly as the ionic fraction of B in the resin increases. A small decrease of K_A^B with increasing X_B can be explained in terms of the changing extent of swelling, but it is impossible to account for the entire effect based on swelling alone. The possible explanation is that resins with a high degree of cross-linking, are micro-heterogeneous in structure, containing regions of different degree of cross-linking. The different regions would take up the competing ions in different proportions, and small amounts of B would go first to sites with greatest affinity for B, whereas less-favorable sites for B would be increasingly difficult to fill. Another explanation is that in some systems, the arrangement ...AAAA..BBBB... may be more stable than ...ABABAB... (in three dimensions) (40).

The Effect of Temperature on Equilibria

The temperature dependence of equilibria is related to the standard enthalpy change which accompanies the process. High temperature discourages the exothermic reaction. The temperature dependence of ion-exchange equilibria is given by the thermodynamic relation

$$\frac{\{d \ln N_{k_B}^A\}}{\{d T\}} = \frac{\Delta H^\circ}{R T^2} \quad (\text{II-18})$$

where $N_{k_B}^A$ is the rational thermodynamic equilibrium constant and ΔH° is the standard enthalpy change for $A + \bar{B} \rightleftharpoons B + \bar{A}$ (27).

Ion-exchange Reactions With The Evolution of Very Small Quantities of Heat. Standard enthalpy changes are usually smaller than 2 kcal/mole. Thus, the temperature dependence of ion-exchange equilibria is usually minor. However, ion exchange may be followed by other processes with considerable enthalpy changes. A common case is the neutralization reaction



Here, the heat of neutralization (13.7 kcal/mole) is liberated, and such systems are more strongly affected by temperature changes (27).

Swelling

Ion exchange resins sorb solvents in which they are placed. While taking up the solvent, the resins expand or swell.

Eventually an equilibrium is attained where swelling ceases. The monomeric units of the resins carry ionogenic groups which tend to

surround themselves with polar solvent molecules. The coiled and packed chains of the matrix unfold and make room for the solvent molecules, but the chains cannot separate completely because they are interconnected by cross-links. As a result, the resins swell, but do not dissolve. Swelling equilibrium is attained when the elastic forces of the resin matrix balance the dissolution tendency.

Swelling equilibria can be accurately described by thermodynamics. These relations, however, involve quantities which cannot be calculated from fundamental data. Therefore, quantitative predictions can be made only when either empirical relations or results of swelling measurements are used.

Swelling Pressure and Solvent Activity

The liquid in the pores of a resin is subject to contractive forces of the matrix and thus under higher pressure than the external solution. The pressure difference between the pore liquid and the solution is called the 'swelling pressure', which is presented as

$$P_s = \bar{P} - P \quad (\text{II-20})$$

where,

P_s = swelling pressure;

\bar{P} = pressure in the resin; and

P = pressure in the external solution.

The swelling pressure affects the solvent uptake and thus the solvent activity in the resin. For a resin in equilibrium with pure solvent (solvent activity in the external phase $a_w = 1$), the following relation is obtained:

$$v_w = - R T \ln \bar{a}_w \quad (\text{II-21})$$

where,

v_w = partial molar volume of the solvent;

a_w = solvent activity in the resin.

Swelling pressures are difficult to measure directly. They are calculated from vapor-sorption isotherms measured with a series of resins of different degrees of cross-linking (Figure 4)(27).

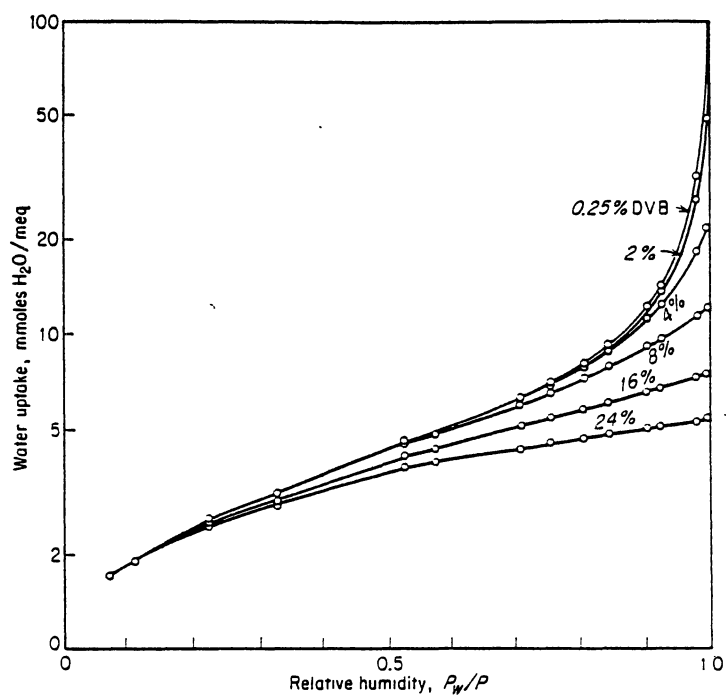


Figure 4. Water-vapor Sorption Isotherms of Ion-exchange Resins. The curves show the water uptake of the hydrogen ions of styrene type cation exchangers of various degrees of cross-linking as a function of the relative humidity of the gas phase (27)

The method of calculation is as follows: two resins of equal structure but with different degrees of cross-linking are compared at equal total gas pressures and equal solvent contents of the resins. The swelling pressure can be calculated using:

$$R T \ln(P_{w1}/P_{w2}) = (P_{s1} - P_{s2}) v_w \quad (\text{II-22})$$

where,

P = saturation vapor pressure of the solvent;

P_w = partial pressure of the solvent; and

1 and 2 refer to the two different resins.

To use Equation (II-22), a weakly crosslinked resin is used for comparison. Another method is to use a series of comparison resins with different degrees of crosslinking and extrapolate to zero crosslinking. Several empirical methods to calculate the swelling pressures are available in literature (27).

Kinetics of Ion Exchange

The theory of ion-exchange kinetics is not as advanced as that of ion-exchange equilibria. The difficulties are mainly mathematical. The problems associated with kinetics are: the mechanism of the process, the rate determining step, whether the rate laws are obeyed, and whether the rate can be predicted theoretically. The first two have been well established, and progress is being made in the other two. The fourth problem is the most difficult to handle. Proposed rate theories have been confirmed using single particle batch studies. Assumptions made in the theories include isothermal systems, uniform spherical particles and insignificant effects of particle swelling and activity coefficient gradients.

The major rate controlling steps are particle and film diffusion. Since these are in series, the slower step is rate controlling. The following theoretical criterion is used to determine the rate controlling step (28):

$$\frac{C \bar{D} \delta}{C_D r_o} (5 + 2 \alpha_B^A) \ll 1 \quad \text{for particle diffusion control} \quad (\text{II-23})$$

and

$$\frac{C \bar{D} \delta}{C_D r_o} (5 + 2 \alpha_B^A) \gg 1 \quad \text{for film diffusion control}$$

where,

C = the total counter-ion concentration (meq/cm³);

D = the effective system diffusivity (cm²/s);

δ = the film thickness (cm);

r_o = the particle radius (cm); and

the bar denotes the resin phase.

The diffusion coefficient within the exchange particle (\bar{D}) must be known to use the above equations. The rate of diffusion within ion-exchangers is not as fast as in solutions due to framework hindrances, tortuous paths, obstruction due to large ions, and ionic interactions with fixed functional groups (53,47). It can be shown that

$$\bar{D} = D(e/(2-e))^2 \quad (\text{II-24})$$

where,

e = the fractional pore volume.

Equation II-24 assumes no blocked or dead end pores and is not accurate for quantitative work. Better correlations are available, based on the degree of cross-linking, external solution concentration, gram equivalent weight of the resin, and the ion diffusion coefficients at infinite dilution in water (33).

In the following discussion of rate theories, a binary exchange between counter-ions A and B will be considered. A is the counter-ion moving from the exchanger and B the counter-ion moving into the exchanger. The co-ion in the solution is designated C (Figure 5).

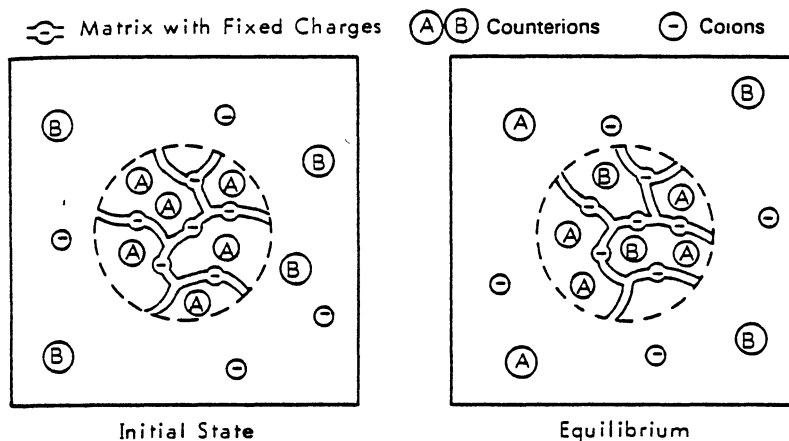


Figure 5. Typical Binary Ion-Exchange System (28)

Particle-Diffusion Control

Due to the preservation of electroneutrality within the particle, we have

$$Z_A \bar{C}_A + Z_B \bar{C}_B = \bar{C} \quad (\text{II-25})$$

$$Z_A \bar{J}_A + Z_B \bar{J}_B = 0 \quad (\text{II-26})$$

where,

\bar{C} = the total concentration of fixed ionic groups in the resin (meq/cm³);

\bar{J}_i = the flux of species i (meq/sec cm²) (25).

The flux is calculated using the Nernst-Planck equation, which includes the ionic effect on the rate in addition to the Fick's Law term.

$$\bar{J}_B = -\bar{D}_B \text{grad}(\bar{C}_B) - \bar{D}_B \bar{C}_B (Z_B F / (R T)) \text{grad}(\phi) \quad (\text{II-27})$$

where,

F = the Faraday's constant (coulombs/mole);

R = the universal gas constant (ergs/mole K);

ϕ = the electrical potential (ergs/coulomb);

D_i = the diffusion coefficient of ionic species (cm²/s); and

T = the absolute temperature (K).

Z_i = ionic charge of species i

Based on the above equations, the effective diffusion coefficient can be derived as

$$\bar{D} = \bar{D}_A \bar{D}_B (Z_A^2 \bar{C}_A + Z_B^2 \bar{C}_B) / (Z_A^2 \bar{C}_A \bar{D}_A + Z_B^2 \bar{C}_B \bar{D}_B). \quad (\text{II-28})$$

The concentration profile and the exchange rate within the exchanger now can be calculated by combining the Equations II-27 with the flux equation $\bar{J}_B = -\bar{D} \text{grad} \bar{C}_B$ and the continuity equation

$$(\delta \bar{C}_B / \delta t) = -\text{div} \bar{J}_B \quad (\text{II-29})$$

and integrating with the proper boundary conditions (28). The primary difficulty here is to solve the partial differential equation (Equation II-19) with the complex boundary conditions. Several attempts to simplify the problem using assumptions have been made (40).

Film Diffusion Control

Film diffusion is more complex than particle diffusion since the effects of co-ions within the film and the hydrodynamic models must be considered. The theoretical models for film diffusion have been developed using the Nernst film concept (40). The particle is assumed to have a completely stagnant film of thickness δ surrounding it with a sharp boundary separating the film layer and the bulk solution. Curvature of the film is neglected, and the film thickness is based on the Sherwood number

$$\delta = 2 r_o / Sh \quad (\text{II-30})$$

where,

Sh = the Sherwood number.

The flux across the film is assumed to be determined as a function of the boundary concentrations (27). The co-ion Y must also be considered in the conditions of electroneutrality and coupled exchange rates.

$$C_A + C_B = C_Y \quad (\text{II-31})$$

and

$$J_A + J_B = J_Y = 0$$

Application of the Nernst-Planck equation to film diffusion has shown excellent qualitative agreement with experimental data. How-

ever, the quantitative agreement has not always been good (65,55,34,73).

To obtain the packed bed mass transfer coefficients (excluding ionic effects), the correlations of Carberry (10) and Kataoka (35) are used. The coefficients calculated this way account for the bed geometry and flow field effects on the mass transfer rate.

$$k_1 = 1.15 (\mu/\epsilon) (Sc)^{-2/3} (Re)^{-1/2} \quad \text{Carberry's equation (11-32)}$$

where,

k_1 = the nonionic liquid phase mass transfer coefficient (cm/s);

ϵ = the bed void fraction;

μ = the superficial liquid velocity (cm/s);

Sc = the Schmidt number; and

Re = the Reynolds number.

$$k_1 = 1.85 (\mu/\epsilon) (\epsilon/(1 - \epsilon))^{1/3} (Sc)^{-2/3} (Re)^{-2/3} \quad \text{Kataoka's Equation (II-33)}$$

The effects of ionic interactions are accounted for by defining a ratio of electrolyte to nonelectrolyte mass transfer coefficient, or by a similarly defined effective diffusivity. This ratio, called the R_i factor is defined by the following expression:

$$R_i = \frac{k_1'}{k_1} = \frac{-D_i \left\{ \frac{\delta C_i}{\delta y} + \frac{Z_i C_i F}{R T} \frac{\delta \phi}{\delta y} \right\}_{y=0}}{-D_i \left\{ \frac{\delta C_i}{\delta y} \right\}_{y=0}} \quad (\text{II-34})$$

here,

y = the distance normal to solid interface (cm); and

k_1' = the ionic liquid phase mass transfer coefficient (cm/s).

The rate of exchange thus can be calculated using Equation II-34.

$$\left\{ \frac{\delta q_i}{\delta t} \right\} = k_1' R_i a_s C_t (x_i^o - x_i^*) \quad (\text{II-35})$$

where,

q_i = the mean resin phase concentration of species i (meq/cm³ resin);

a_s = the specific surface area (cm² area/cm³ resin); and

the superscript o denotes value in the bulk phase.

The ionic effects can also be accounted for by defining an effective ionic liquid phase diffusivity (D_e). This effective diffusivity is related to the ratio of ionic to nonionic mass transfer coefficients by (25)

$$(D_e/D_B)^{2/3} = (k_1'/k_1) = R_i \quad (\text{II-36})$$

Thus, the rate of exchange can be determined using

$$(\delta q_i/\delta t) = k_1' (D_e/D_B)^{2/3} a_s C_t (x_i^o - x_i^*) \quad (\text{II-37})$$

Simplified differential equations have often been used due to their simplicity of integration (17,30):

$$(\delta \bar{C}_B/\delta t) = k_1' a_s (C_B^o - C_B^*) \quad (\text{II-38})$$

and

$$k_1' = D/\delta \quad (\text{II-39})$$

Some type of average system diffusivity (D), which is between the diffusion coefficients for the two exchanging species, is normally used. In some cases, the linear driving force model has given quantitative results comparable to those given by the Nernst-Planck equation (58,29).

Ion Exchange Accompanied by Reaction

An ion-exchange process may be followed by a chemical reaction. A cation exchanger in the hydrogen form contacted with a sodium hydroxide solution will be accompanied by a neutralization reaction. The hydrogen ions leaving the exchanger immediately react with the hydroxide co-ion at the particle surface. For rates controlled by particle diffusion, the reaction will not affect the diffusion or rate of exchange within the particle, and Equation II-28 is valid. However, the boundary condition at the particle surface will be affected. Solutions for particle-diffusion control and with $C_A = 0$ at the exchanger interface have been tabulated (58,29).

When the exchange rate is controlled by film diffusion, an accompanying reaction has a significant effect on the flux equations. To satisfy electroneutrality,

$$C_H + C_{Na} = C_{OH} \quad (\text{II-40})$$

Thus,

$$C_H < C_{OH} \quad (\text{II-41})$$

in the film. Since the hydrogen and hydroxide ions are linked by the ionic product expression (25°C):

$$C_H C_{OH} = K_w = 10^{-14} \text{ mole}^2/\text{lit}^2 \quad (\text{II-42})$$

the effective system diffusivity (D) can be shown to be:

$$D = 2 D_{Na} D_{OH} / (D_{Na} + D_{OH}) \quad (II-43)$$

and analytical solutions for various systems have been derived (28).

Model for Mixed-Bed Ion-Exchange

The mixed-bed ion-exchange model (25) used as the basis of this work, is based on the theory of liquid resistance controlled reactive ion-exchange at low solution concentrations. The cation and anion resins are treated separately. This permits the study of the following effects: variation of the cation and anion resin ratio; differing cation and anion exchange rates; exchange capacities; and particle sizes. The other effects considered are: reversibility of exchange at low concentrations, neutralization reactions within the film and bulk liquid phases, and effluent ion concentrations of the order of one part per billion (1×10^{-7} M). These considerations are included in the model by accounting for the position of the neutralization reaction front and the water dissociation constant in separate flux equations for the cation and anion resins. The flux equations in the model are based on the Nernst-Planck Theory (Equation II-27) in conjunction with the static film hydrodynamic model and nonionic mass transfer coefficient correlations for packed beds (Equations II-32 and II-33) (25).

The derived ion flux expressions do not account for particle diffusion resistance within the exchange resins. Other assumptions in the model are: uniform bulk liquid and surface compositions for a given exchange particle, equilibrium at the particle-film interface, fast neutralization reactions compared to the rate of exchange, activity coefficients of unity for the concentrations studied, pseudo steady state mass transfer across the film layer, isothermal system,

and negligible dispersion in the mixed bed. The above assumptions can be shown to be reasonable (25).

Temperature Dependent Terms in the Model

The temperature dependent quantities in the mixed-bed ion-exchange model are: resin selectivity coefficients, ionic diffusion coefficients, ionization constant of water, and viscosity of the bulk solution. The effect of temperature on these quantities is discussed in this section.

Resin Selectivity Coefficients

The temperature dependency of the selectivity coefficient can be obtained from the various theoretical models describing ion-exchange equilibria. The simplest and most useful model was introduced by Gregor (20,21). According to this model, the matrix of the resin is a network of elastic springs. When the resin swells, the network is stretched and exerts a pressure on the internal pore liquid (Figure 6). The swelling pressure in the resin affects swelling, sorption, and ion-exchange equilibria. In the thermodynamic treatment of this model, the components of the system are usually taken to be the matrix with fixed ionic groups, the various mobile ionic species, and the solvent. This model explains the selectivity sequence of the alkali ions and other rules in systems in which the swelling pressure effect is not obscured by other forces. Only the purely mechanical swelling pressure is considered. Electrostatic interactions are not included. Lazare and Gregor suggested a model considering the effect of electrostatic interactions (46).

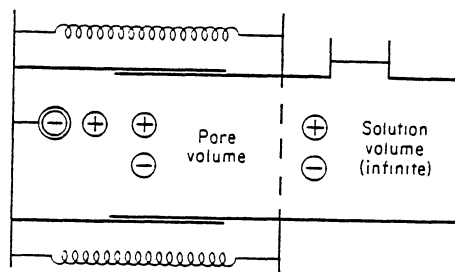


Figure 6. Gregor's Model of the Ion Exchanger (28)

A variety of approaches and models have been developed for predicting selectivity coefficients. The conclusions derived from these models are diverse. The models proposed by Katchalsky and by Harris and Rice are based on considerations on a molecular scale (37,38,51,60,62). Flory, Rehner and Kuhn developed models based on configurational entropy computed by use of the statistical theory of the elasticity of nonpolar, macro-molecular networks (14).

In the simplest and most clear treatment of ion-exchange equilibria, the elastic matrix model (Gregor's) is used. This model leads to the relation

$$E_{\text{Don}} = (R T \ln(a_i/a_i^-) - P_s v_i)/(z_i F) \quad (\text{II-44})$$

where,

E_{Don} = Donnan Potential

z_i = electrochemical valence of species i

F = Faraday constant

a_i = activity of species i

P_s = swelling pressure (atm.)

v_i = partial molar volume of species i (cm^3).

Equation (II-44) holds for any mobile species, irrespective of the number of species present in the system. When applied to the counter-ion, Equation (II-44) reflects the dependence of the Donnan potential on the concentration (or activity) difference between the ion-exchanger and the solution and on the counter-ion valence. When applied to the co-ion, Equation (II-44) shows the dependence of co-ion exclusion on the Donnan potential and on the co-ion valence.

The application of Equation (II-44) to the exchange of a strong electrolyte, AY, by an ion-exchanger in form A requires the following relations. One mole of the electrolyte dissociates to give n_A moles of ions A and n_Y moles of ions Y (A is the counter-ion and Y the co-ion). Hence,

$$z_A n_A = -z_Y n_Y \quad (\text{II-45})$$

and the partial molar volume of the electrolyte is

$$v_{AY} = n_A v_A + n_Y v_Y \quad (\text{II-46})$$

Combining the equations (II-4) for both the mobile species A and Y with equations (II-45) and (II-46), we have

$$R T \ln\left(\frac{a_A}{a_A} \frac{a_Y}{a_Y}\right)^{n_A n_Y} = P_s v_{AY} \quad (\text{II-47})$$

Now, considering the two competing counter-ions A and B, we get

$$R T \ln\left(\frac{a_A}{a_A} \frac{a_B}{a_B}\right)^{z_B z_A} = P_s (z_Z v_B - z_B v_A) \quad (\text{II-48})$$

Substituting the activities by molalities m_i according to

$$a_i = m_i \gamma_i \quad (\text{II-49})$$

and using the definition of the selectivity coefficient, we have

$$\ln K_B^A = \ln (\bar{\gamma}_B^{z_A} / \bar{\gamma}_A^{z_B}) + \ln (\gamma_A^{z_B} / \gamma_B^{z_A}) + P_s (z_A v_B - z_B v_A) / (R T) \quad (\text{II-50})$$

Evaluation of Terms in Equation for Selectivity

The swelling pressure may be computed from vapor-sorption isotherms, and using Equation (II-22) described earlier. A similar method described by Boyd and Soldano (7) is to use the relation

$$P_s = (R T / v_w) \ln (a_{w1} / a_{w2}) N_m \quad (\text{II-51})$$

where,

N_m = weight normality of the resin

v_w = partial molal volume of water in the resin

a_{w1} = activity of water in the resin

a_{w2} = activity of water in a chemically identical unlinked resin containing the same amount of water per equivalent.

$\ln a_{w1}$ can be calculated from known osmotic coefficients, ϕ , at the concentration of the electrolyte. $\ln a_{w2}$ for an unlinked resin of the same normality (N_m), as the cross-linked resin can be interpolated from the values of $\ln a_w$ determined on a very weakly cross-linked exchanger as a function of N_m in isopiestic vapor pressure measurements (27). A small correction to the value of P_s estimated from Equation (II-51) is made for the pressure P_o , in the weakly cross-linked exchanger when it is in equilibrium with pure water using

$$P_o = (R T M_w / 1000 \bar{v}_w) v \phi^o N_m \quad (\text{II-52})$$

where,

M_w = the molar mass

$v \phi^o$ = molal osmotic coefficient

N_m^o = weight normality of the fully swollen exchange.

The value of $v\phi^0$ can be calculated by extrapolating the experimentally determined curve for the variation of $v\phi^0$ with N_m to N_m^0 .

A least squares fit to relate the activity coefficients to the weight normalities of the form

$$N_m = \alpha + \beta(-\ln a_w) + \delta(-\ln a_w)^2 \quad (\text{II-53})$$

can be obtained. Equation (II-53) can be applied in several ways in the computation of second and third terms in Equation (II-50)(65).

The partial molal volume difference, $(z_A v_B - z_B v_A)$ can be calculated from experimental measurements of the equivalent volumes, V_e , of resins of varying water content and ionic composition by (52).

$$(v_B - v_A) = (V_B - V_A) - (\delta \bar{v}_w / \delta x_A) x_w dx_w \quad (\text{II-54})$$

where,

V_A and V_B = molar volumes of the dry resins A and B respectively

x_A = equivalent fraction of A (i.e. the loading)

x_w = equivalent water content.

An empirical fit to calculate the $(V_B - V_A)$ term, can be used to ease calculations (65). Experimental values of the equivalent volumes, V_{eA} for varying values of x_A and x_w can be fitted to the equation

$$V_{eA} = V_A + c x_w^2 / (b + x_w) \quad (\text{II-55})$$

where,

V_A = equivalent volume of the dry exchanger

b, c = parameters of the least squares fit.

The first term of the right hand member of Equation (II-50) reflects the contribution of the ionic interactions in the exchanger to the

selectivity coefficient. It can be evaluated by means of Equation (II-56) from measurements of the variation of x_w for a weakly cross-linked exchanger with ionic composition.

$$\ln (\bar{\gamma}_B/\bar{\gamma}_A) - \ln (\bar{\gamma}_B/\bar{\gamma}_A)^* = 0.05551 \int_0^{\ln a_w} (\delta x_w/\delta x_A)_{a_w} d \ln a_w \quad (\text{II-56})$$

To facilitate the calculation of the term $(\delta x_w/\delta x_2)$, a least squares equation of the form

$$x_w = a + b x_A + c x_A^2 \quad (-\ln a_w \text{ Constant}) \quad (\text{II-57})$$

can be obtained. To estimate the term $\ln (\bar{\gamma}_B/\bar{\gamma}_A)^*$, an experimental measurement of the selectivity coefficient on the same exchanger at infinite dilution is obtained. This corresponds to zero swelling pressure and gives:

$$\ln K_B^{A*} = \ln (\gamma_B/\gamma_A)^* \quad (\text{II-58})$$

The accurate evaluation of $\ln K_B^{A*}$ requires that the measured values of $\ln K_B^{A*}$ be extrapolated to infinite dilution, and corrected for the fact that pressure is not zero. Neglect of these refinements introduces an error well below that of the measurements themselves. The term for the mean molal ionic activity coefficient ratio for the dilute mixed electrolyte can be evaluated following the method of Robinson and Stokes (22), given by

$$\ln (\gamma_B/\gamma_A) = \ln (\gamma_B^0/\gamma_A^0) - (b_1 - b_2)m \quad (\text{II-59})$$

where,

γ_B^0 and γ_A^0 are the activity coefficients for electrolytes B and A when present alone in aqueous solution at molality m , and the parameters b_1 and b_2 are related to available tabulated constants in literature (22).

The assumptions in the above method of calculation to evaluate the terms are: The Donnan invasion of cross-linked exchangers by electrolyte is neglected. At high electrolyte concentrations or for weakly cross-linked exchangers, electrolyte penetration may become appreciable, and Equation (II-56) will become inapplicable.

Examination of Equation (II-56) shows that a calculation of $\ln(\bar{\gamma}_B/\bar{\gamma}_A)$ on an absolute basis cannot be accomplished. Selectivity coefficients estimated with Equation (II-50) will be relative to those for the weakly cross-linked exchanger upon which the isopiestic weight swelling measurements were made. An absolute measurement can be realized when $\ln K_B^A = \ln(\bar{\gamma}_B/\bar{\gamma}_A) = 0$. This is true for the exchange of sodium with hydrogen ions and with several alkali metal cations (52). However, with strong-base-anion exchangers large selectivity coefficients are observed, even with the most lightly cross-linked preparations. Equation (II-50) assumes that the properties of highly cross-linked exchangers may be estimated from measurements on a very weakly cross-linked exchanger. It is thus assumed that cross linking does not change the thermodynamic properties, so that all exchangers of the same chemical type and exchange capacity will show the same values of $\ln(\bar{\gamma}_B/\bar{\gamma}_A)$ and $(z_A v_B - z_B v_A)$ if they are of identical weight swelling.

CHAPTER III

INTRODUCING TEMPERATURE EFFECTS

The mixed-bed ion-exchange model of Haub and Foutch (25) assumes uniform isothermal conditions of 25° C throughout the bed. This work allows the use of the model between 10° and 90° C. These temperature limits are fixed by the range of temperature (10-90° C here) in which the selectivity coefficients are correlated by the method of least squares. The new model calculates all parameters at T° C (the operating temperature). No provisions are made to consider the variation of temperature with column height, i.e., the column is assumed to operate isothermally at T° C. The parameters in the model affected by temperature are:

1. resin selectivity coefficients,
2. ionic diffusion coefficients,
3. ionization constant for water, and
4. viscosity of the bulk solution phase.

Effect of Temperature on the Selectivity Coefficient

Ion exchange is an exothermic process. Thus, high temperature adversely affects ion-exchange equilibria (and hence, the selectivity coefficient). The effect of temperature on some common ion-exchange processes is illustrated in Tables I and II. A significant decrease in the selectivity coefficients with increase in temperature is seen.

TABLE I
 VARIATION OF SELECTIVITY COEFFICIENT WITH
 TEMPERATURE ON 16% DVB DOWEX-50
 RESIN (4)

T(°C)	K_{H}^{Na}	$K_{H}^{NH_4}$	K_{H}^{Tl}	K_{Mg}^{Cu}	K_{Cu}^{Ca}
0	1.97	2.58	24.2	1.31	1.38
25	1.55	2.13	15.7	1.28	1.36
50	1.42	1.87	11.8	1.23	1.34
77	1.33	1.66	8.95	1.20	1.32
97.5	1.24	1.54	7.89	1.17	1.31

TABLE II
 COMPARISON OF CALCULATED AND OBSERVED VALUES
 FOR CUPRIC-HYDROGEN EXCHANGE ON
 16% DOWEX-50 RESIN (5)

T(°C)	K_{H}^{Cu} (Calculated)	K_{H}^{Cu} (Observed)
0	2.59	2.56
25	2.69	2.68
50	2.82	2.90
77	3.01	3.10
97.5	3.14	3.27

Correlating Temperature to Selectivity

Selectivity coefficients can be related to their controlling parameters by theoretical models developed by Gregor (20), Lazare and Gregor (46), Katchalsky (37), Rice and Harris (24), Myers and Boyd (52), Kielland (39), Gaines and Thomas and (16), Pauley (57). All these models are based on fundamental thermodynamics. Most of these models are complex and present formidable problems in evaluating model parameters.

Gregor's Model

The simplest and widely used model is that by Gregor, based on the Gibbs-Donnan equilibrium (Equation II-50). This has been extensively studied and applied to several ion-exchange systems. The match between experimental and theoretical results using Gregor's model is good. Such comparisons between experimental and theoretical values are shown in Tables II, III, and IV.

Method of Kraus and Raridon

Using the Debye-Huckel theory for electrolytes, Kraus and Raridon (41) developed a method for expressing selectivity coefficients as functions of temperature. The activity coefficients in the aqueous phase are calculated using the Debye-Huckel equation in this method. Kraus and Raridon showed that if the heat capacity changes are assumed to be constant, the expression for the selectivity coefficient is:

$$\log K = \log K_t + C' \log(T/T_t) + C''(1 - (T_t/T)) \quad (\text{III-1})$$

where, C' ; C'' and K_t are constants and subscript "t" refers to a reference temperature (41).

TABLE III

SELECTIVITY COEFFICIENTS FOR THE EXCHANGE OF TETRAMETHYL-AMMONIUM WITH SODIUM ION FOR VARIOUS EQUIVALENT FRACTIONS (x_{TMA}) OF 2, 4, 8% DVB CROSSLINKED POLYSTYRENE SULFONATE (41)

% DVB	x_{TMA}	$K_{\text{calculated}}$	K_{observed}
2	0.00	1.38	1.34
	0.50	1.28	1.13
	1.00	1.09	0.94
4	0.00	1.14	1.23
	0.50	0.89	0.86
	1.00	0.58	0.60
8	0.00	0.81	0.92
	0.50	0.66	0.58
	1.00	0.53	0.48

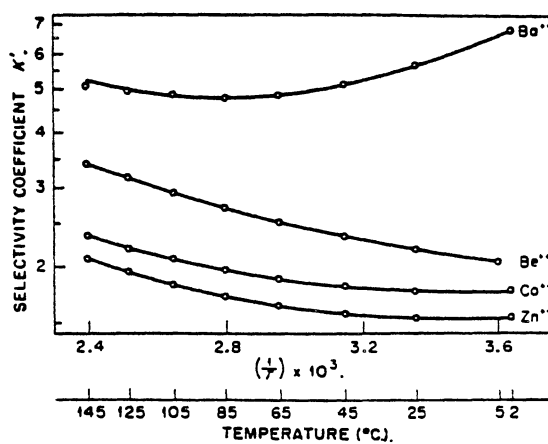


Figure 7. Temperature Dependence of Cation-exchange Equilibria (Metal Tracers on Dowex-50 Resin, H⁺ form)(41)

TABLE IV
 SELECTIVITY COEFFICIENTS FOR VARIOUS COMPOSITIONS
 AND DEGREES OF CROSSLINKING IN THE SODIUM-
 LITHIUM ION-EXCHANGE SYSTEM (52)

% DVB	x_{Na}	$K_{calculated}$	$K_{observed}$
2	0.0	1.28	1.12
	0.5	1.24	1.10
	1.0	1.21	1.08
4	0.0	1.56	1.40
	0.5	1.50	1.44
	1.0	1.46	1.48
8	0.0	2.0	1.72
	0.5	1.88	1.80
	1.0	1.72	1.89
12	0.0	2.45	2.15
	0.5	2.33	2.05
	1.0	2.20	1.95
16	0.0	2.56	2.40
	0.5	2.48	2.13
	1.0	2.39	1.88
24	0.0	3.34	3.75
	0.5	2.92	2.40
	1.0	2.80	1.80

TABLE V
PARAMETERS IN KRAUS-RARIDON EQUATION (41)

A. Hydrogen-form resin					
Ion	$\log K_t$	C'	$-C''$	C_p	T_{\min}
Na^+	0.019	4.683	2.437	9.3	144
K^+	0.454	5.735	3.474	11.4	213
Rb^+	0.467	5.694	3.868	11.3	271
Cs^+	0.574	7.811	5.042	15.5	244
Be^{++}	0.417	2.884	0.686	5.7	-82
B. Sodium-form resin					
K^+	0.244	0.564	0.777	1.1	800
Rb^+	0.312	0.209	0.745	0.4	>1000
Cs^+	0.427	0.441	1.02	0.9	>1000

By fitting experimental data to Equation III-1 by the method of least squares, the parameters (C' , C'' and K_t) listed in Table V can be obtained. The deviations between observed and calculated values of the selectivity coefficient (Table VI) appear to be within limits of experimental error except in a few cases at the extremes of the temperature range.

TABLE VI

COMPARISON OF OBSERVED AND CALCULATED VALUES OF SELECTIVITY COEFFICIENTS AS A FUNCTION OF TEMPERATURE BASED ON THE METHOD OF KRAUS AND RARIDON (42)

T(°C)	K_{Na}^H		K_K^H		K_{Rb}^H	
	obsd.	calc.	obsd.	calc.	obsd.	calc.
5	1.51	1.50	not available		7.65	7.68
25	1.29	1.30	4.46	4.47	5.44	5.40
45	1.15	1.16	3.62	3.61	4.05	4.06
65	1.08	1.08	3.04	3.05	3.23	3.23

Other methods of correlating the temperature dependency of selectivity coefficients have been reported (3,8,9,12,32,43,44,50,56,59,64,68,72, however neither of them are easy to use nor have been extensively studied. For practical purposes, the Gregor's model and the Kraus-Raridon method provide convenient and powerful practical methods for determining the effect of temperature on equilibria.

Factors Affecting Resin Behavior

Resin properties depend on the following factors:

1. Type of resin used - chemical groups in the resin, degree of crosslinking and method of preparation of the resin.
2. Initial relative proportion of ions in the resin and bulk solution phase.
3. Chemical nature of counter-ions A and B.

4. Other substances present in the solution phase, for example, other reacting or non-reacting ions.
5. Temperature.

Selectivity of ion-exchange resins is enhanced by increasing their degree of crosslinking and by decreasing the solution concentration. Ions with higher valence; smaller (solvated) equivalent volume and greater polarizability are preferred. The effect of the degree of crosslinking on the selectivity is illustrated in Tables III and IV.

Thus, each resin exhibits a unique behavior depending on the above five factors. In an effort to compare the mixed-bed ion-exchange behavior at various temperatures between 15° and 70° C, the following equations for the cation and the anion exchange resins were used in the Haub & Foutch model.

$$K_{\text{Na}}^{\text{H}} = 1.1814 + 9.9836/T - 9.195/T^2 \quad (\text{III-2})$$

$$K_{\text{Cl}}^{\text{OH}} = 1.2031 + 6.1505/T + 6.2143/T^2 \quad (\text{III-3})$$

Both the equations (III-2 and III-3) were obtained by applying the method of least squares to experimental data. The equation for the cation-exchange selectivity coefficient was developed by using experimental results reported on 16% DVB Dowex exchanger (5). This resin has a selectivity coefficient of 1.55 at 25° C (the value used in the Haub & Foutch model). Data on anion-exchange resins is rather scarce compared to cation-exchange resins. The Haub & Foutch model used a selectivity coefficient of 1.45 for the anion-exchange resin. Since, no anion-exchange resin seen in literature gave a selectivity of

1.45 at 25° C, Equation III-3 was fictitiously generated. The cation-exchange selectivity coefficient was first plotted as shown in Figure 10. The anion-exchange plot was then drawn keeping the value of selectivity coefficient of 1.45 at 25° C. The rest of the curve for the anion-exchange resin was arbitrarily drawn. Any anion exchange resin is bound to behave in an analogous manner to the behavior depicted in Figure 10. A specific resin used can be described accordingly by either using experimental data fitted by the method of least squares or by the theoretical methods of Gregor and Kraus-Raridon.

Effect of Temperature on Ionic Diffusion Coefficients

In an electrolyte solution the solute is in the form of cations and anions. Because the size of the ions are different than the original molecule, their mobility through the solvent is different. The smaller ion diffuses faster than the larger ion. However, so that a separation of electric charge does not occur, both ionic species must diffuse at the same rate.

The Nernst equation (31) provides a simple and accurate method for predicting diffusion coefficients in electrolyte solutions by relating the diffusion coefficient to electrical conductivities.

$$D_{AB}^{\circ} = \left\{ \frac{R T}{F^2} \right\} \left\{ \frac{\lambda_{+}^{\circ} \lambda_{-}^{\circ}}{\lambda_{+}^{\circ} + \lambda_{-}^{\circ}} \right\} \left\{ \frac{Z_{-} + Z_{+}}{Z_{+} Z_{-}} \right\} \quad (\text{III-4})$$

where,

F = Faraday constant, A.s/g-equiv.,

D_{AB}° = diffusion coefficient at infinite dilution, m^2/s ,

λ_{+}° = cationic conductance at infinite dilution, $(A/cm^2) (cm/V)$
(cm^3/g -equiv.),

λ_{-}° = anionic conductance at infinite dilution, (A/cm²) (cm/V)
(cm³/g-equiv.),

$\lambda_{+}^{\circ} + \lambda_{-}^{\circ}$ = electrolyte conductance at infinite dilution, (A/cm²) (cm/V)
(cm³/g-equiv.),

R = universal gas constant

Z_{+} = cation valence

Z_{-} = anion valence

T = absolute temperature, °K.

The Nernst equation has been verified experimentally for dilute solutions.

The diffusion coefficients of single ions in solution can be calculated using:

$$D_i^{\circ} = (R T/F^2) \lambda_i^{\circ} \quad (\text{III-5})$$

where,

λ_i° = the equivalent conductance of ionic species i at infinite dilution (63) and the superscript 'o' refers to infinite dilution.

Equation III-5 provides a convenient method of relating temperature to the ionic diffusion coefficients.

The conductance of electrolytes increases with temperature (49). The variation of equivalent conductance with temperature can be represented by the equation

$$\lambda_t^{\circ} = \lambda_{25^{\circ}\text{C}}^{\circ} (1 + \beta(t-25)) \quad (\text{III-6})$$

where,

λ_t° = equivalent conductance at t°C,

λ_{25}° = equivalent conductance at 25°C,

β = a constant, 0.022-0.025 for salts and 0.016-0.019 for acids.

The variation of the equivalent conductance with temperature at infinite dilution for some ions is illustrated in Table VII (63).

TABLE VII
VARIATION OF EQUIVALENT CONDUCTANCE WITH
TEMPERATURE AT INFINITE DILUTION (63)

Ion	Limiting Equivalent Conductances, λ_i° of ions in water at various temperatures ($^{\circ}\text{C}$)					
	5 $^{\circ}$	18 $^{\circ}$	25 $^{\circ}$	45 $^{\circ}$	55 $^{\circ}$	100 $^{\circ}$
H $^{+}$	250.1	315.0	349.8	441.4	483.1	630.0
OH $^{-}$	---	171.0	198.6	---	---	450.0
Na $^{+}$	30.3	42.8	50.10	73.7	86.8	145.0
Cl $^{-}$	47.5	66.0	76.35	108.9	126.4	212.0

To express the diffusion coefficient of ions as a function of temperature, Equation III-5 and Table VII can be used. The data in Table VII was used here to correlate temperature and the equivalent conductance at infinite dilution using the method of least squares. The equations obtained are:

$$\lambda_{\text{H}}^{\circ} = 221.7134 + 5.52964T - 0.014445T^2 \quad (\text{III-7})$$

$$\lambda_{\text{OH}}^{\circ} = 104.74113 + 3.807544T - 0.00355T^2 \quad (\text{III-8})$$

$$\lambda_{\text{Na}}^{\circ} = 23.00498 + 1.06416T + 0.0033196T^2 \quad (\text{III-9})$$

$$\lambda_{\text{Cl}}^{\circ} = 39.6493 + 1.39176T + 0.0033196T^2 \quad (\text{III-10})$$

Combining Equations III-5 to III-10 provides an expression for relating the effect of temperature on the diffusion coefficients of ions. The final equations are of the form

$$D_i = (RT/F^2)(A_i + B_i T + C_i T^2) \quad (\text{III-11})$$

where,

A_i , B_i and C_i are the least square fit parameters. Equations of the form III-11 have been used in this work to express the variations of the ionic diffusion coefficients as a function of temperature.

Effect of Temperature on Ionization Constant of Water

Many equations have been proposed to represent the temperature variations of the ionization constant, but the methods used to evaluate the constants in the equations imposes severe restrictions on their applicability. The most accurate equations are based on experimental methods. The experimental results are a set of cell potentials measured at regularly spaced temperature intervals. These can be represented within experimental error by a quadratic least square fit in temperature. By ordinary thermodynamic methods, the relation between the ionization constant and temperature can be derived as (23)

$$R \ln K_{IP} = -A/T + B - CT$$

where,

R = universal gas constant

K_{IP} = ionization constant

A, B, C = constants

T = temperature

Many of the proposed equations to express the ionization constant as a function of temperature reproduce the experimental data well. However, Equation III-11 is more closely related to the experimental results and is therefore adequate as a compact method to fit experimental data.

Water is a very weak acid and the determination of its ionization constant requires special methods. The ionization constant of water can be represented by (23)

$$-\log K_w = 4470.99/T - 6.0875 + 0.01706T \quad (\text{III-12})$$

Equation III-12 has been used in this model.

Effect of Temperature on Viscosity of the Bulk Solution Phase

Methods for the direct calculations of liquid viscosities based on theoretical methods have not yet been developed and empirical estimation techniques need to be used. These methods do not conflict with theory, they merely allow some of the unknown or incalculable theoretical constants to be approximated empirically from structure or other physical properties (61).

The viscosity of liquids decreases with temperature. Over a wide range of temperatures from above the normal boiling point to near the freezing point, the viscosity - temperature plots can be represented by the Andrade Correlation (61).

$$\mu_1 = A \exp (B/T) \quad (\text{III-13})$$

where,

μ_1 = liquid viscosity (CP)

T = liquid temperature

A,B = constants of the Andrade correlation.

Several other empirical viscosity temperature relations have been suggested (61). One form shown to be accurate at low temperatures is,

$$\mu_1 = \exp (B/(T + C)) \quad (\text{III-14})$$

Regardless of the many suggested modifications, Equation III-13 is still the most widely used equation for correlating temperature to liquid viscosity.

For a number of associated liquids, Makhija and Stairs (48) tabulated the parameters A', B', and T' for use in their equation, of the form:

$$\mu_1 = \exp (A' + B' / (T-T')) \quad (\text{III-15})$$

where,

μ_1 = liquid viscosity, CP

T = absolute temperature, °K

Constants A', B', T' for some polar liquids are given in Table VIII.

TABLE VIII
POLAR LIQUID VISCOSITIES

Liquid	A'	B'	T'	% error	Range (°C)
Water	-1.5668	230.298	146.797	0.51	-10 to +160
Ethanol	-2.4401	774.414	-15.249	2.66	-98 to +70
Ammonia	-1.7520	218.76	50.701	0.76	-69 to +40
n-Butanol	-3.0037	1033.306	-4.3828	0.80	-51 to +100

A more recent correlation to express the dynamic viscosity of water as a function of temperature is (13)

$$\log \mu_1 = -1.64744 + 262.37/(T-133.98) \quad (\text{III-16})$$

where,

μ_1 = liquid viscosity (CP)

T = absolute temperature ($^{\circ}\text{K}$)

Extensive experimental viscosity-temperature data for sodium chloride solutions are now available (13). However, since the salt concentrations in the water entering mixed-bed ion-exchange columns is very low (10^{-7} - 10^{-8} molar), the solution can be treated as pure water for calculating the viscosity. Equation (III-15) has been used here to express the effect of temperature on the viscosity of the bulk solution phase.

CHAPTER IV

RESULTS AND DISCUSSION

The effect of temperature on the temperature dependent parameters is shown in Figures 8, 9, 10, and 11. The selectivity coefficient and the solution viscosity decrease as temperature is increased. The ionization constant of water and the ionic diffusion coefficients increase with increase in temperature. The overall effect of temperature on the mixed-bed behavior is due to the temperature dependency of the above mentioned four parameters.

Figures 12 to 16 show the effect of temperature on the sodium and chloride concentration profiles after 6, 57, and 97 minutes, for a cation/anion ratio of 1.5. The concentration profiles after 6 minutes show that higher temperature results in lower effluent concentrations, indicating that exchange is better at higher temperatures. The concentration profiles after 57 and 97 minutes have two zones. Closer to the column inlet, the higher temperature curves give higher effluent concentration. However, farther from the column inlet, the situation is reversed. Thus, near the column inlet, where the ratio of effluent to feed solution concentration is high, ion exchange is impaired at higher temperatures, but after a certain low effluent concentration is reached, the exchange is better and continues to be for the entire remaining portion of the column.

Figures 17 and 18 show the concentration profiles for bulk phase neutralization and for neutralization in the liquid film respectively.

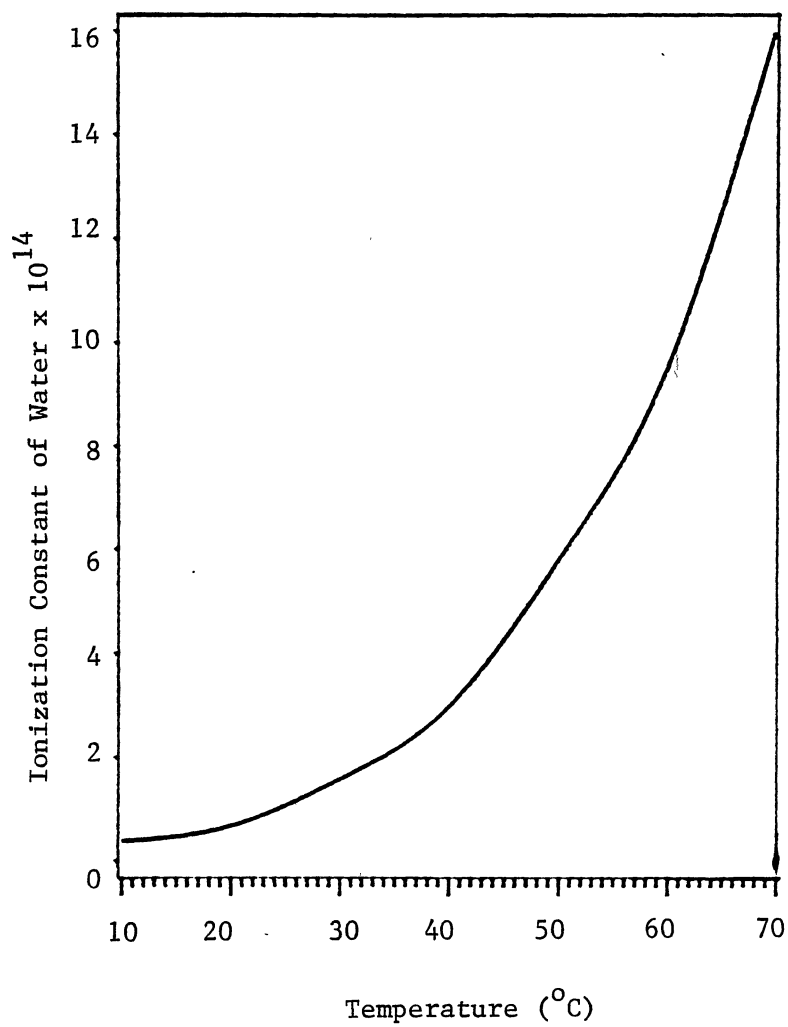


Figure 8. Variation of Ionization Constant of Water with Temperature

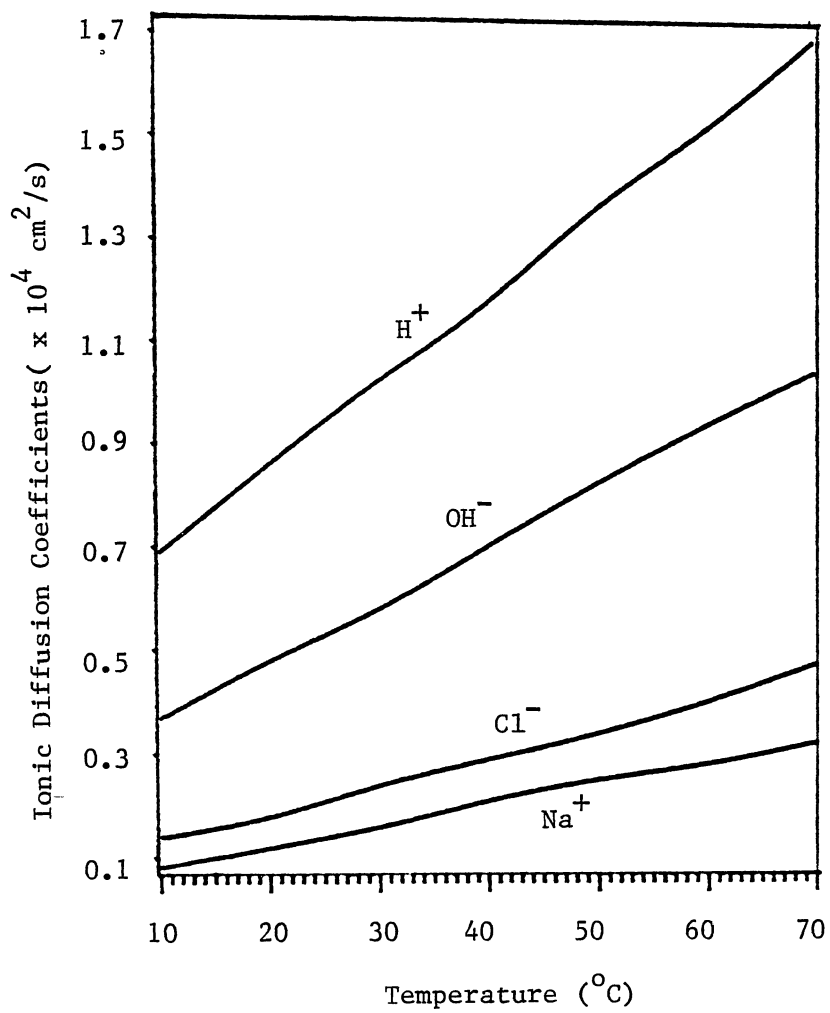


Figure 9. Variation of Ionic Diffusion Coefficients with Temperature

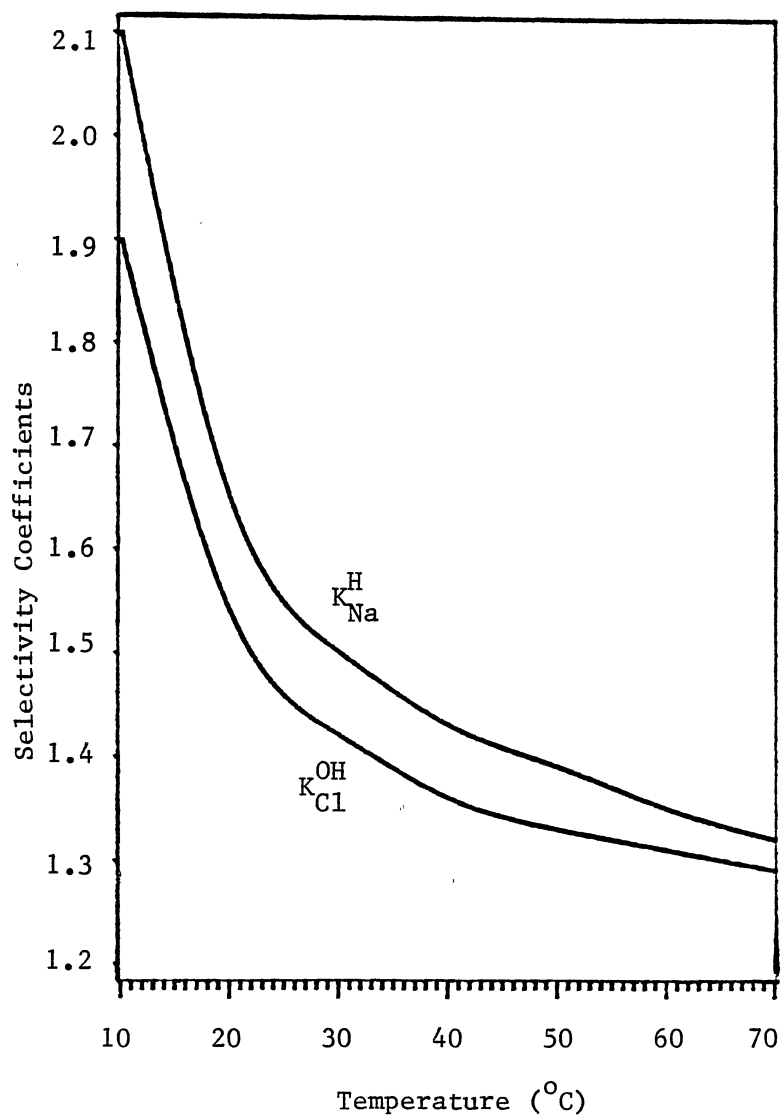


Figure 10. Variation of Cationic and Anionic Selectivity Coefficients with Temperature

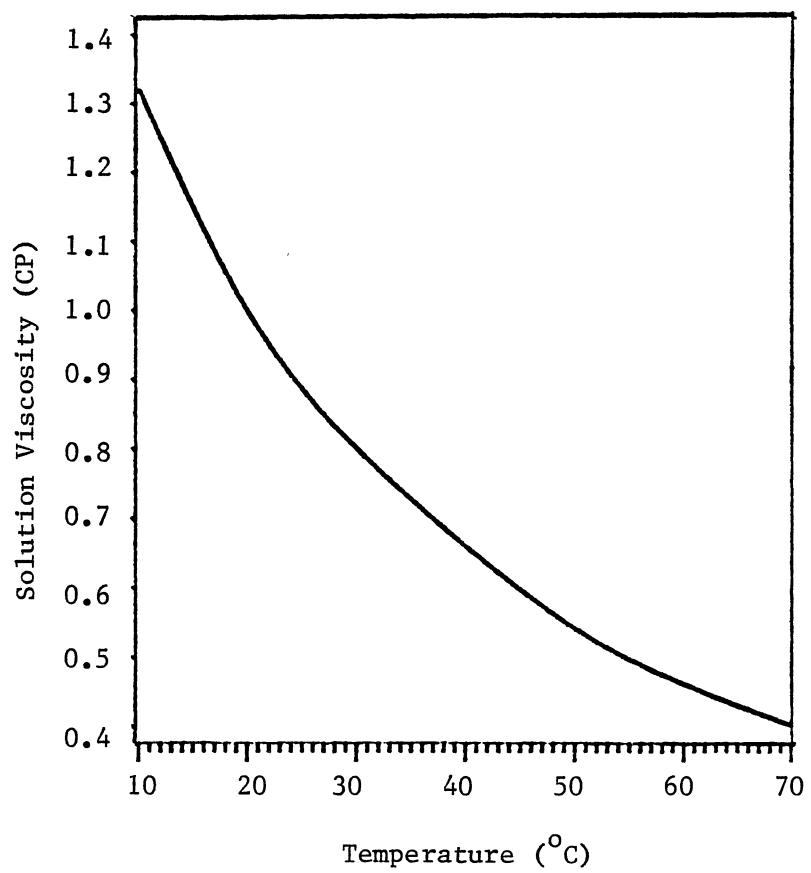


Figure 11. Variation of Solution Viscosity with Temperature

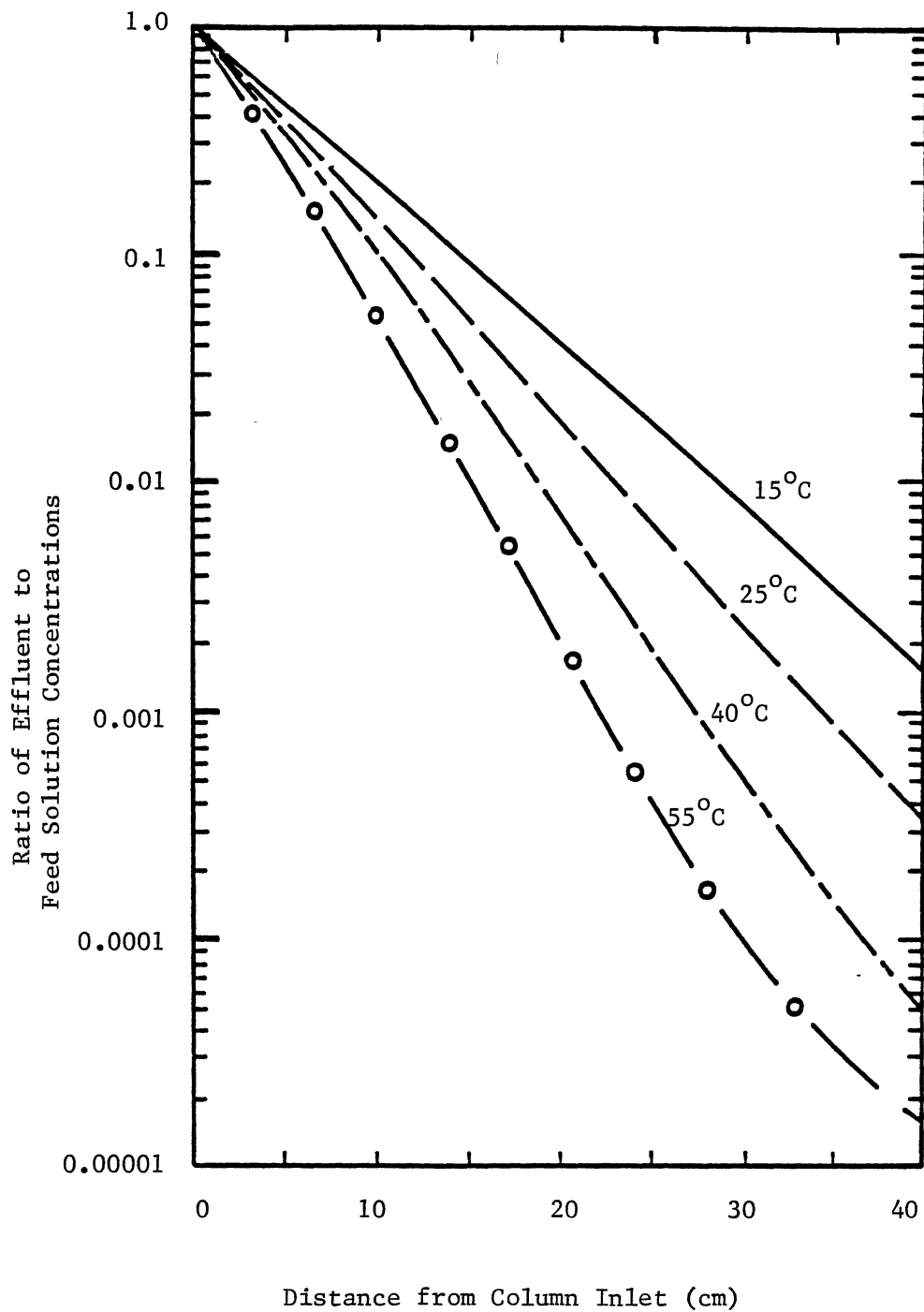


Figure 12. Variation of Sodium and Chloride Concentration Profiles with Temperature After 6 min. and Cation/Anion Ratio = 1.5

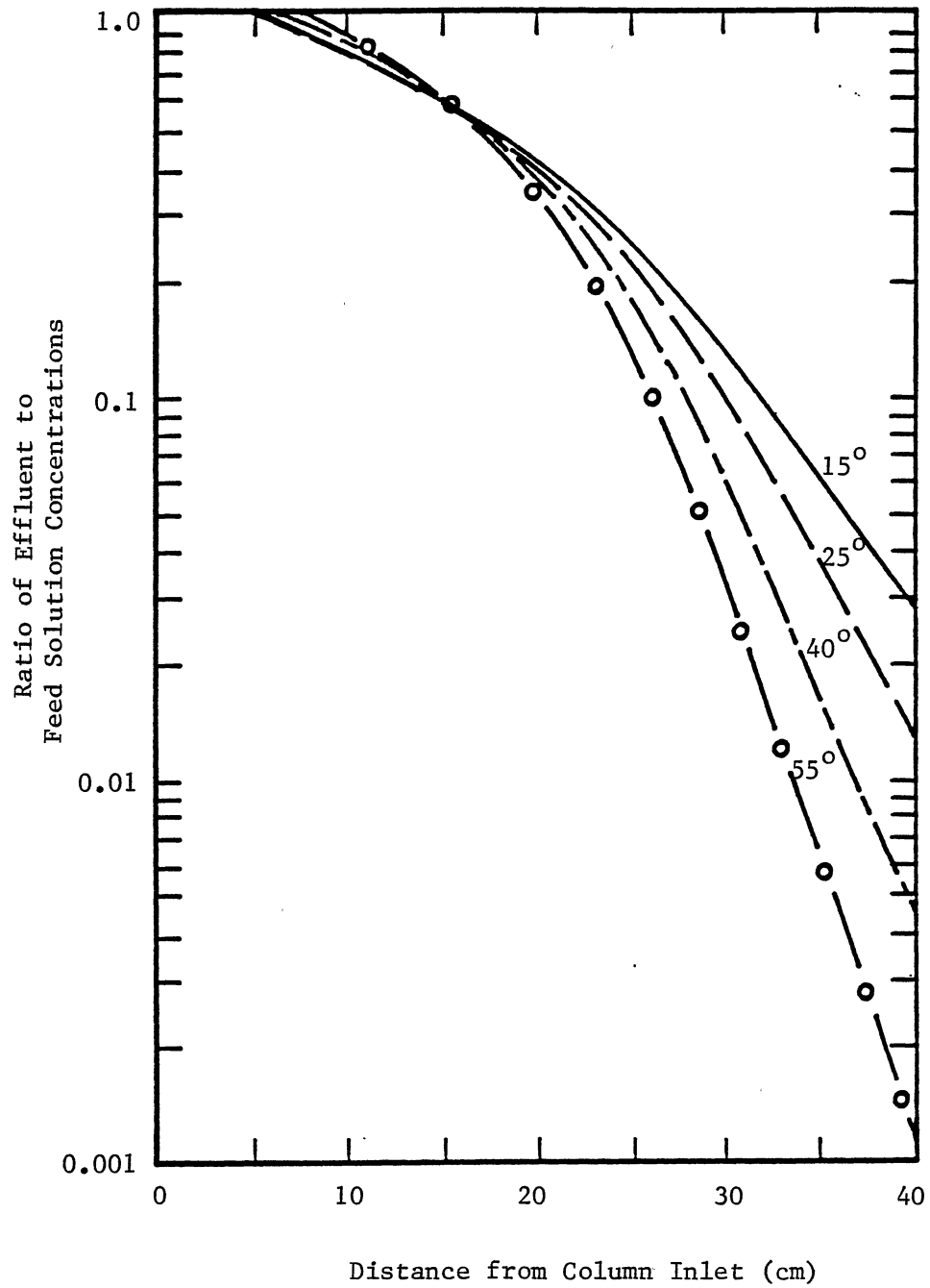


Figure 13. Variation of Sodium Concentration Profiles with Temperature after 57 min. and for Cation/Anion Ratio of 1.5

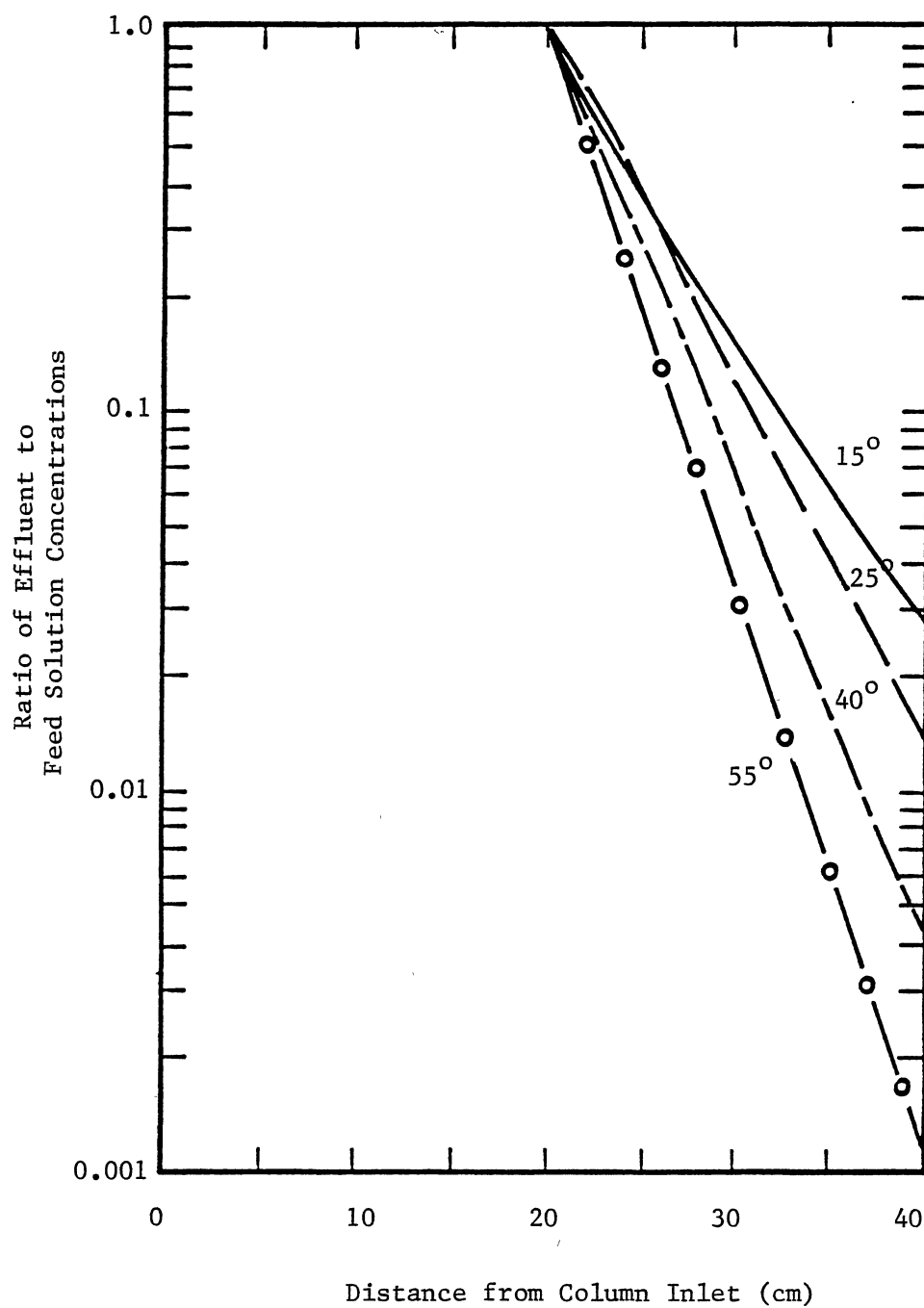


Figure 14. Variation of Chloride Concentration Profiles with Temperature after 57 min. and for Cation/Anion Ratio of 1.5

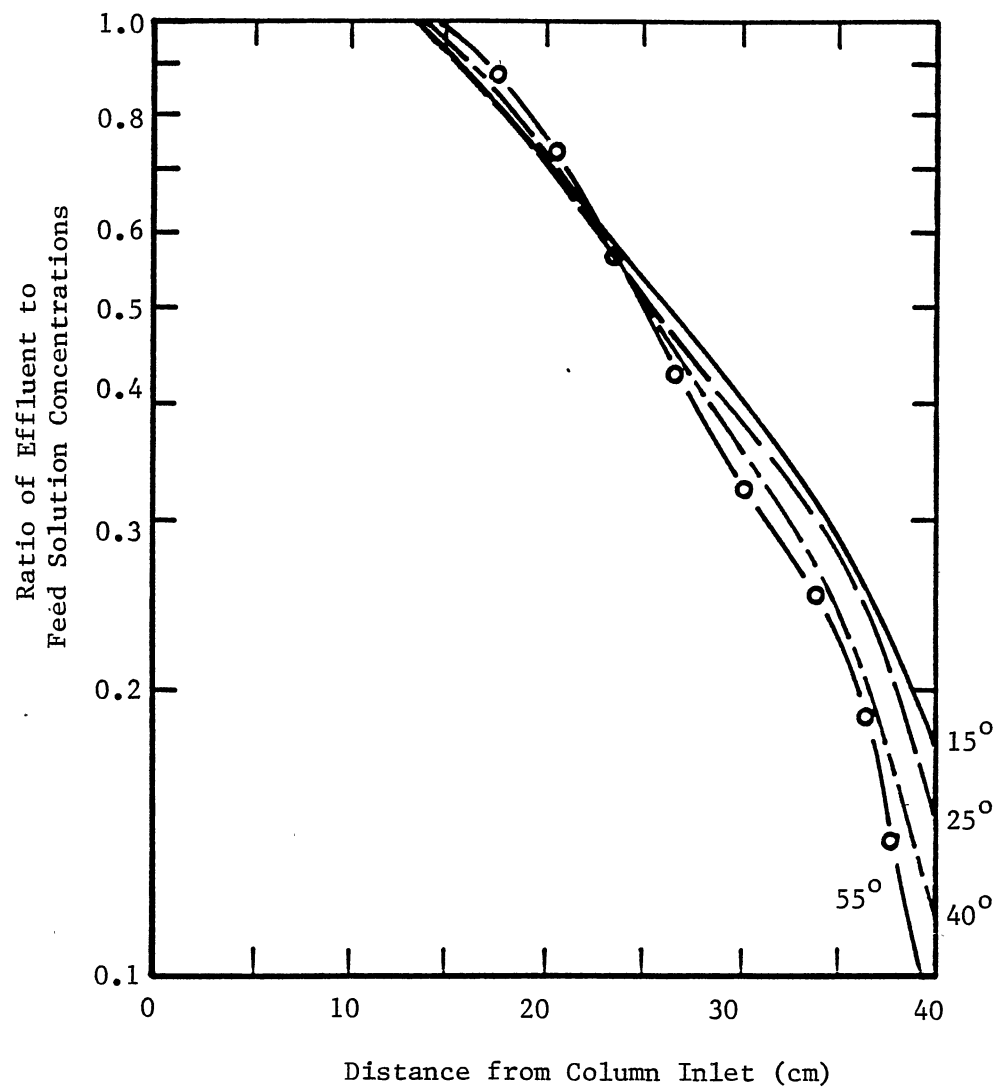


Figure 15. Variation of Sodium Concentration Profile with Temperature after 97 min. and for Cation/Anion Ratio of 1.5

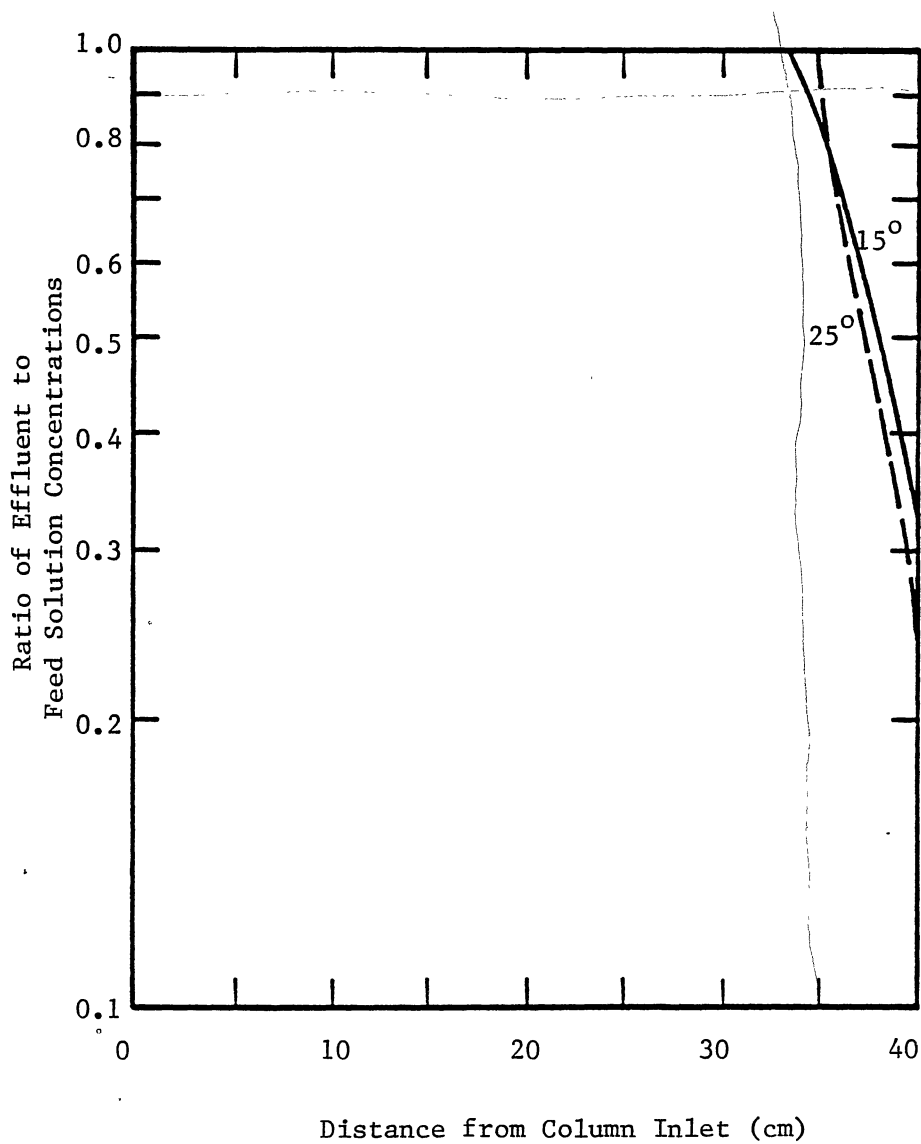


Figure 16. Variation of Chloride Concentration Profile with Temperature after 97 min. and for Cation/Anion Ratio of 1.5

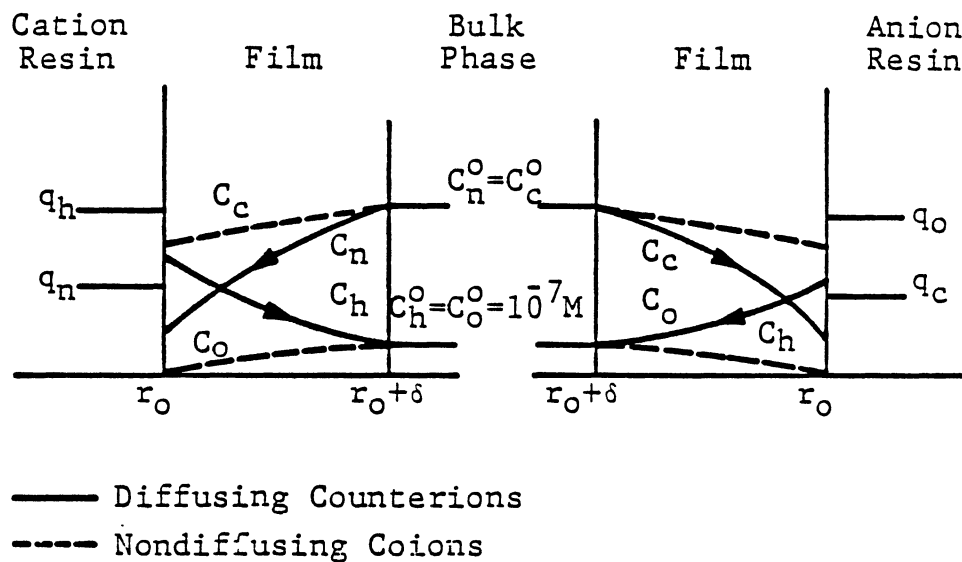


Figure 17. Concentration Profiles for Mixed-Bed Ion-Exchange with Neutralization in the Bulk Phase

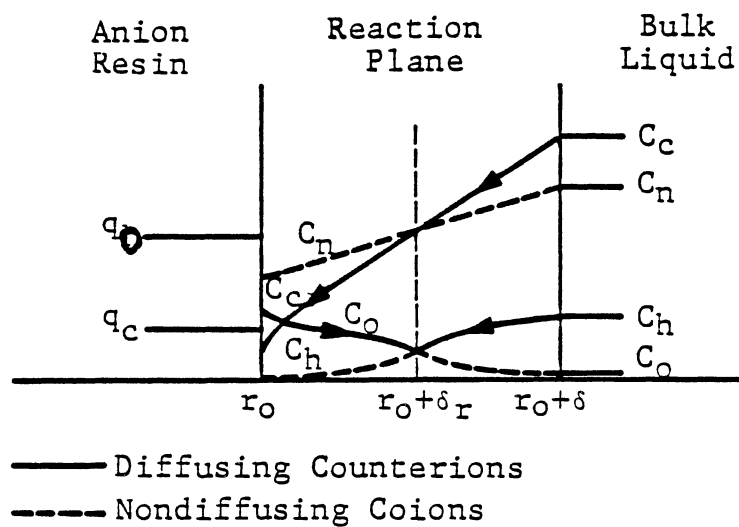


Figure 18. Concentration Profiles for Anion Exchanger with Neutralization in the Liquid Film

As temperature is increased, the selectivity coefficients steadily decline, whereas, the ionization constant of water and the ionic diffusion coefficients increase. The ionization constant shows a twenty-fold increase from 15° to 70° C. The ionic diffusion coefficients increase by a factor of three in this range. The other parameters change to a much smaller extent. Thus, the most pronounced effect due to a temperature change is in the ionization constant. At higher temperatures, both C_h and C_o (the hydrogen and hydroxyl ion concentrations) are increased due to the increase in the ionization constant of water. This results in a reduced concentration gradient for the mass transfer of the hydrogen and hydroxyl ions. Thus, the flux for mass transfer of the hydrogen and hydroxyl ions is controlled by two opposing factors. The diffusion coefficients tend to increase the flux but the increased bulk phase concentrations tend to reduce the flux. If the latter effect is dominating, the mass transfer of the hydrogen and hydroxide is impaired. Since ion-exchange is a stoichiometric process, this reduces the flux of the ions diffusing out of the resins. The behavior of the process based on the concentration profiles can be thus explained on the basis of the above discussion. The concentration profiles after 6 minutes do not show the two clear zones seen for 57 and 97 minutes. However, in the very near vicinity of the column inlet, a small region may exist, giving better exchange at higher temperatures. Investigating the process at the column inlet with very small distance increments may reveal this zone.

The breakthrough curves (Figures 19 and 20) for sodium and chloride exhibit identical trends as explained above. The breakthrough

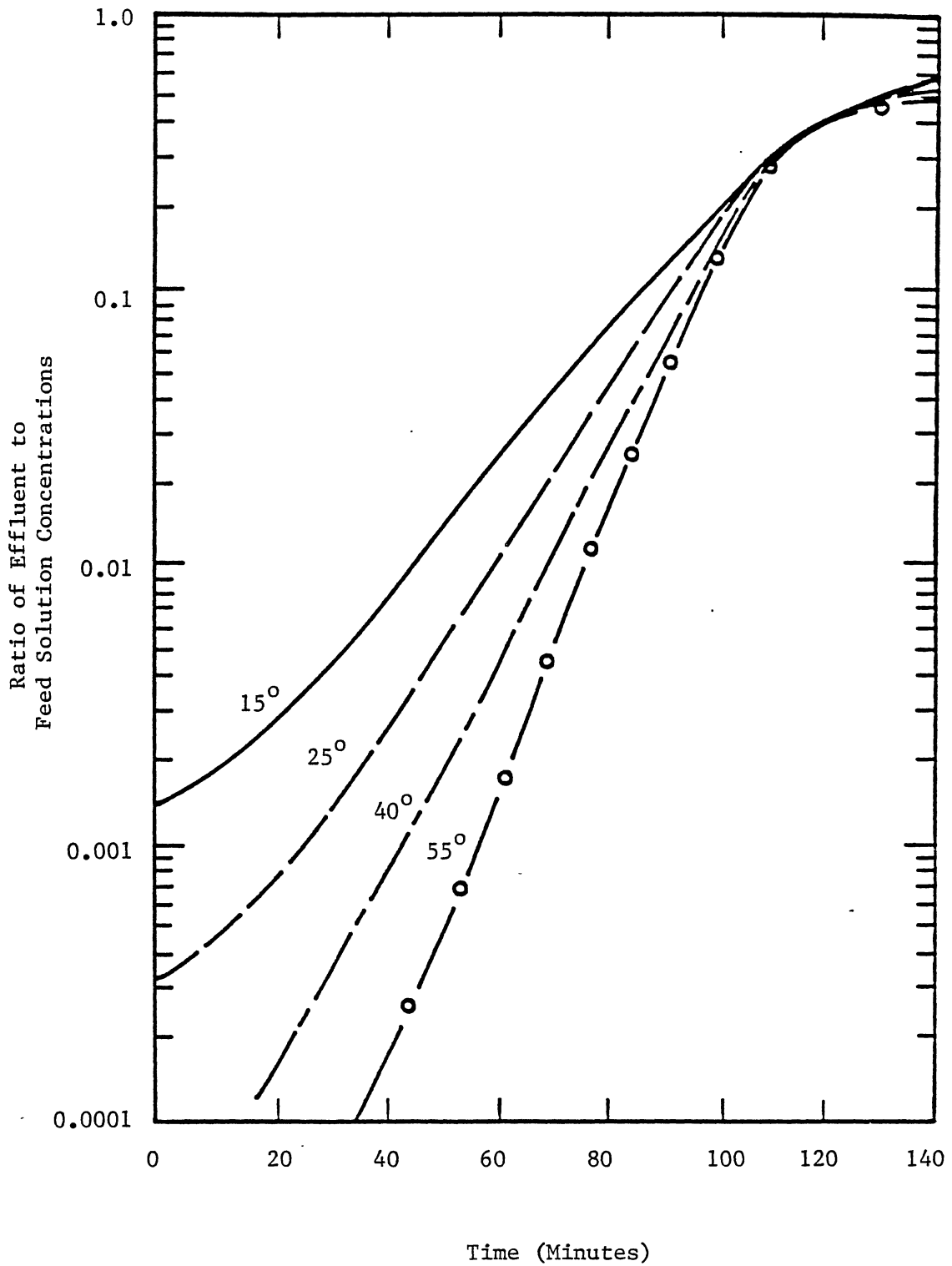


Figure 19. Sodium Breakthrough Curves for Mixed-Bed Simulations with Temperature for Cation/Anion Ratio of 1.5

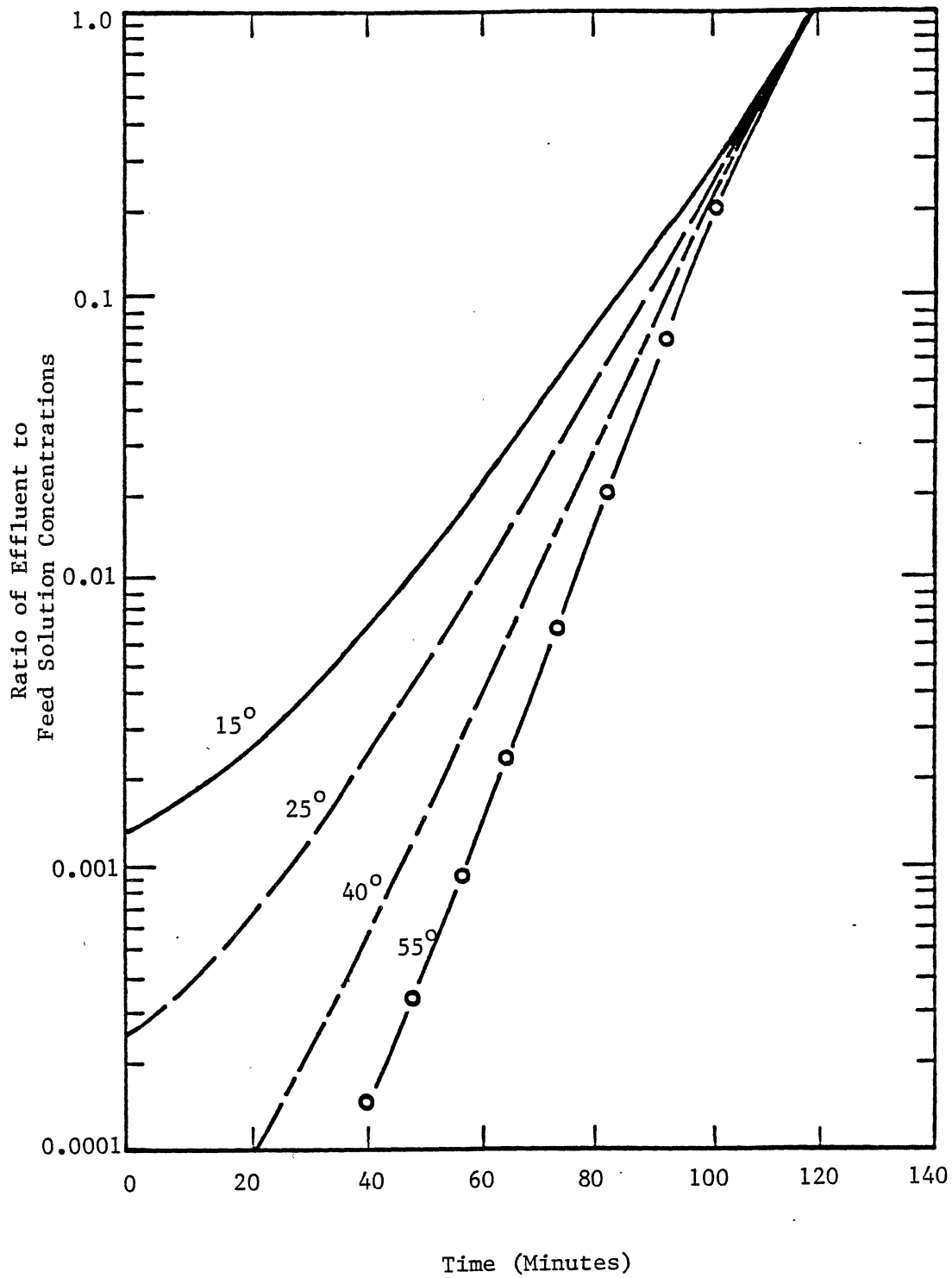


Figure 20. Chloride Breakthrough Curves for Mixed-Bed Simulations with Temperature for Cation/Anion Ratio of 1.5

curves are steeper at higher temperatures. The ratios of the effluent to feed solution concentrations differ by two orders of magnitude between the temperature range of 15° to 55° C. Again, at high ratios of effluent to feed solution concentrations, a reverse effect is noticed. The breakthrough curves, thus improve at higher ratios. At earlier times, higher temperatures give a smaller effluent to feed solution concentration ratio. Near saturation, the situation reverses, higher temperatures giving higher effluent concentrations. This can be explained again on the basis of the discussion above, namely the opposing effects of the ionic diffusion coefficients and the concentration gradients. The important feature in Figures 19 and 20 is that though higher temperatures produce lower values of the effluent to feed solution concentration (better exchange), near the saturation limit, all curves almost coincide, lower temperatures being just marginally better. In the case of the chloride breakthrough profiles, the same trend is noticed, though this difference is even less, compared to the sodium breakthrough profiles. All profiles almost completely overlap as saturation is approached. However, again at higher temperatures, lower values of the effluent to feed solution concentrations, are obtained before resin exhaustion.

Figures 21 and 22 show the effect of temperature on the rate of exchange as a function of the equivalent fraction of chloride in the resin phase. At equilibrium, the concentrations at the particle-solution interface equal those in the bulk phase. There exists a short period near the establishment of equilibrium in which the concentration gradients level out as the interface neutralization reaction diminishes. This period has not been accounted for by any of the available models, including the Haub and Foutch model. This results

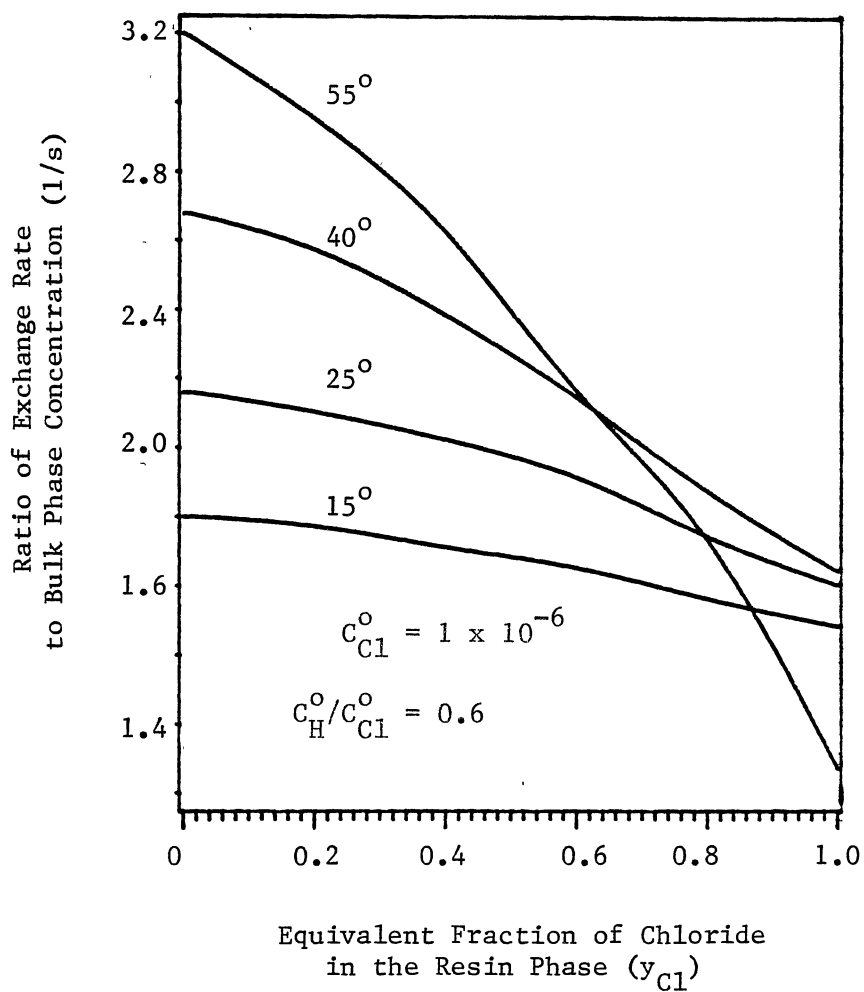


Figure 21. Variation of Exchange Rate with Bulk Phase Concentration and Progress of Ion-Exchange (Film Reaction Model)

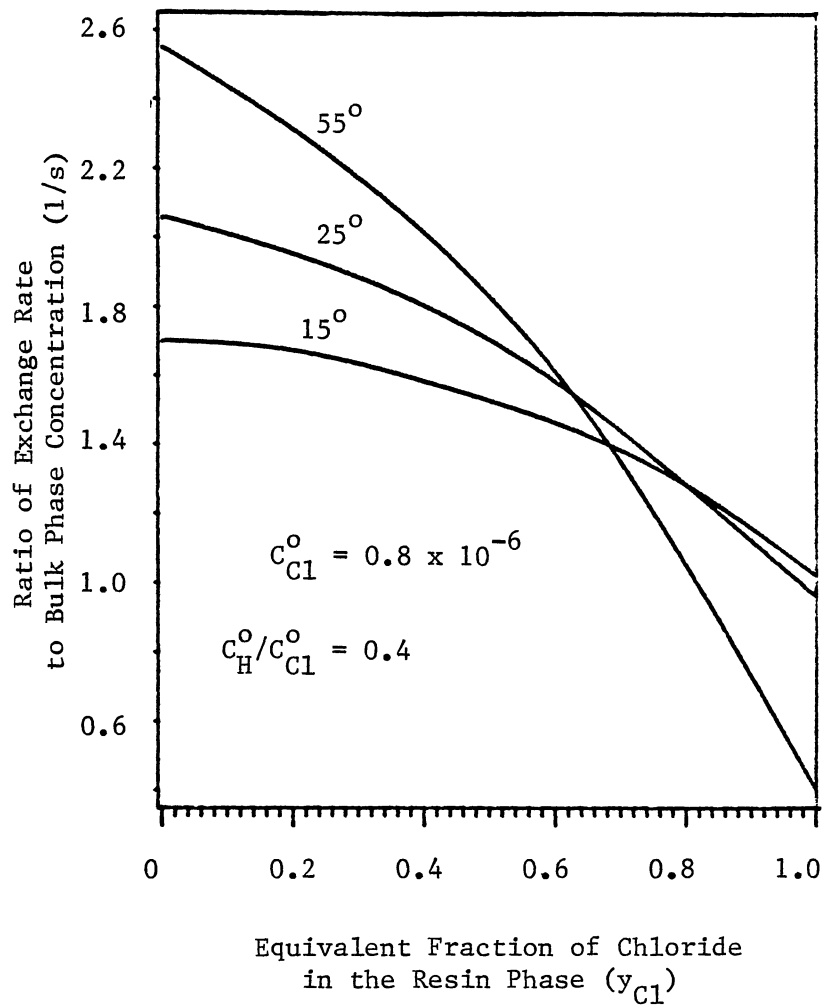


Figure 22. Variation of Exchange Rate with Bulk Phase Concentration and Progress of Ion-Exchange (Film Reaction Model)

in a finite rate of exchange at equilibrium. The effect of increase in temperature is to increase the exchange rate. The increase in rate at higher temperatures can be attributed to the improved mass transfer coefficients. The non-ionic mass transfer coefficients are calculated using Kataoka's and Carberry's correlations (Equations II-32 and II-33). Due to the significant decrease in the solution viscosity at higher temperatures, the mass transfer coefficients are increased. The viscosity effect completely cancels the effect of decreased selectivity coefficients and reduced concentration differences. The R_i factors are also seen to increase with temperature in a certain zone as seen in Figure 23. Even in the zone of reduction of R_i factors with increased temperature, the effect of mass transfer coefficients is dominating. The overall result is the increase of rate with increase in temperature at low solution concentrations. Figure 23 illustrates the effect of temperature on the ratio of electrolyte to nonelectrolyte mass transfer coefficient as a function of the equivalent fraction of chloride in the resin phase. The ratio R_i is a measure of the ionic interaction. The R_i factor as seen from Figure 23 is strongly dependent on temperature. At lower temperatures and at low values of the chloride concentrations in the resin phase, the R_i factors are higher than their corresponding higher temperature values. A certain chloride concentration in the resin phase, a crossover point is seen, where higher temperatures give higher R_i values. The high R_i values at higher temperatures can be attributed to the high hydrogen ion concentration due to the increased ionization constant of water. The low R_i values at high temperatures and low chloride concentrations in the resin phase are due to the reduced concentration gradients and higher values of diffusivities.

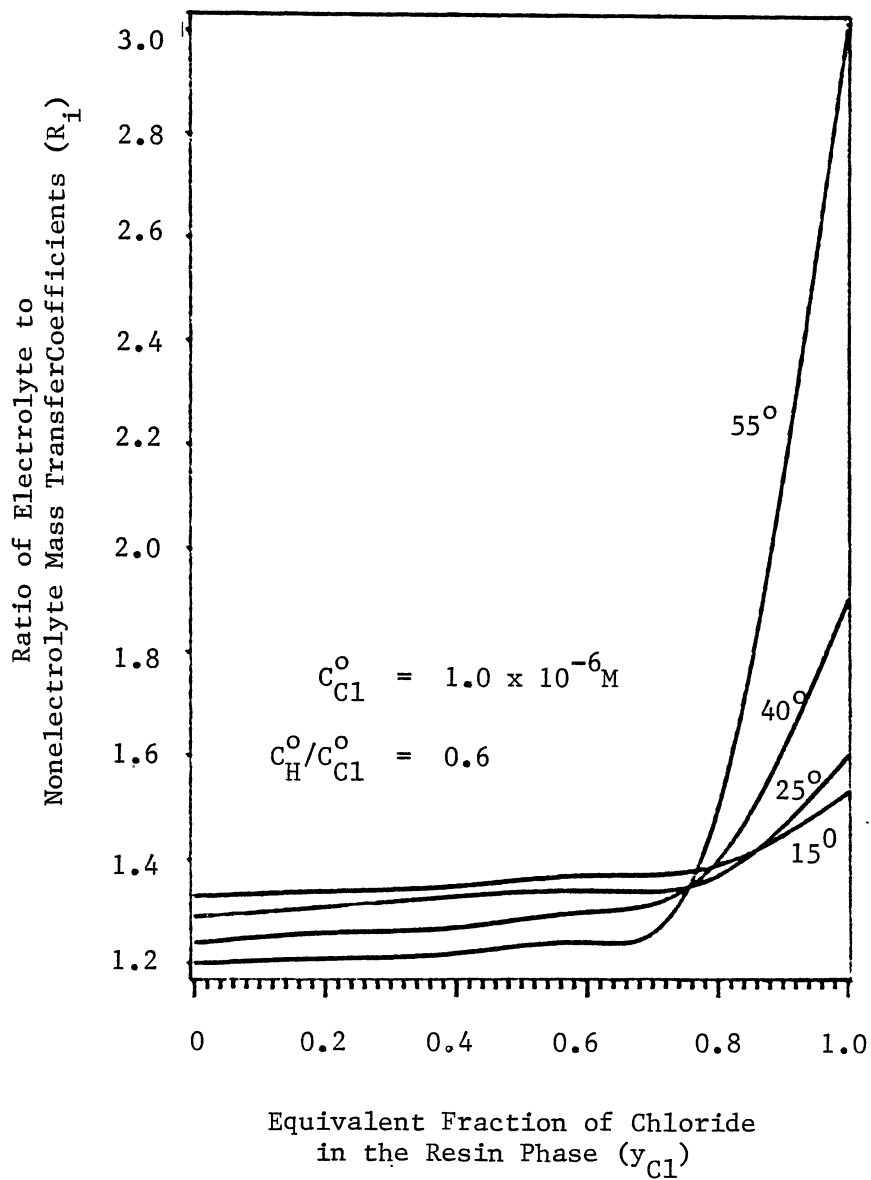


Figure 23. Variation of R_i with Bulk Phase Concentration and Progress of Ion-Exchange for $C_{Cl}^o = 1 \times 10^{-6} M$ (Film Reaction Model)

CHAPTER V

CONCLUSIONS AND RECOMMENDATIONS

Conclusions

The aim of this thesis was to: (a) extend the current liquid resistance controlled reactive mixed-bed ion-exchange model to consider the effect of temperature, and (b) study the results and predictions of the model and compare with available experimental data. The major points from this study are summarized below.

Temperature Dependent Parameters

The four temperature dependent parameters (resin selectivity coefficients, ionic diffusion coefficients, ionization constant of water and viscosity of the bulk solution phase) have opposing overall effects on the ion-exchange phenomenon. The most important temperature dependent factor is the ionization constant of water, which shows a sixteen fold increase as temperature is increased from 10° C to 60° C. The ionic diffusion coefficients exhibit a three fold increase in this temperature range. The remaining two factors, resin selectivity coefficient and the solution viscosity, decrease with increase in temperature. The resin selectivity coefficients are reduced by a factor of 1.5 and the viscosity by a factor of three. Thus, two parameters show a significant increase with temperature whereas, the remaining two show a slight decrease. Due to these opposing factors,

it is not possible to conclude a priori whether temperature is likely to have a favorable or unfavorable effect on mixed-bed ion-exchange phenomenon. However, based on the results and simulations at several temperatures, it is possible to conclude the following:

1. The ionization constant of water and the ionic diffusion coefficients cause the most significant changes in the mixed-bed ion-exchange behavior.

2. The decrease in resin selectivity coefficient with increase in temperature is over-ridden by the above two factors.

3. The effect of the decrease in solution viscosity (with temperature increase) on the mixed-bed behavior is difficult to interpret qualitatively based on the results. The solution viscosity has a direct influence on the mass transfer coefficients (and hence the R_i factors) and also on transport of ions. The resulting effect on the mixed-bed performance is a complex function of these variables.

4. An important effect due to the increase in the ionization constant of water and the diffusion coefficients is seen in the concentration profiles and breakthrough curves clearly. Two distinct zones are seen. In one zone, higher temperature gives better results, in the other, the reverse effect is noticed.

5. The breakthrough limits at exhaustion are only marginally affected by temperature, as seen from Figures 12-17 and 19-20. However, the effect of temperature at lower effluent concentrations and earlier times is strong. Thus, temperature is an important parameter in mixed-bed ion-exchange particularly so, because column operation is terminated and the resins subjected to regeneration well below complete exhaustion of the resins.

Recommendations

The following recommendations are made concerning extensions of this model and areas of future work.

1. This work considered the column operation at uniform temperature at all points in the column. The flux equations can be modified to consider variation of temperature along the column height. Based on the heats of the ion-exchange reaction, the temperature variation along the column height can be determined. Ion-exchange processes however, are accompanied by small exothermic heats and hence, no significant changes may be expected.

2. The mixed-bed ion-exchange model could be rigorously tested by experimental methods to check for its accuracy. A possible experimental set up is illustrated in Figure 24. The feed solution enters the top of the mixed-bed column containing pure regenerated cation and anion resins. The entire column can be either jacketed or covered with heating tape for maintaining it at desired temperatures. The U-bend ensures the complete wetting of the resins. The column is designed with small ports along its height through which samples can be withdrawn for analysis. At the end of the ion-exchange cycle, the cation and anion resins are separated by density difference (gravity method). A neutral substance in the form of beads having an intermediate density can be used to ensure thorough separation. The separated cation and anion exchange resins can be now regenerated in a separate column by contacting them with measured strengths of hydrochloric acid and sodium hydroxide. Analysis and experimental techniques are described in detail by several researchers (5,21,42). A simple jacketed column set-up is illustrated in Figure 25.

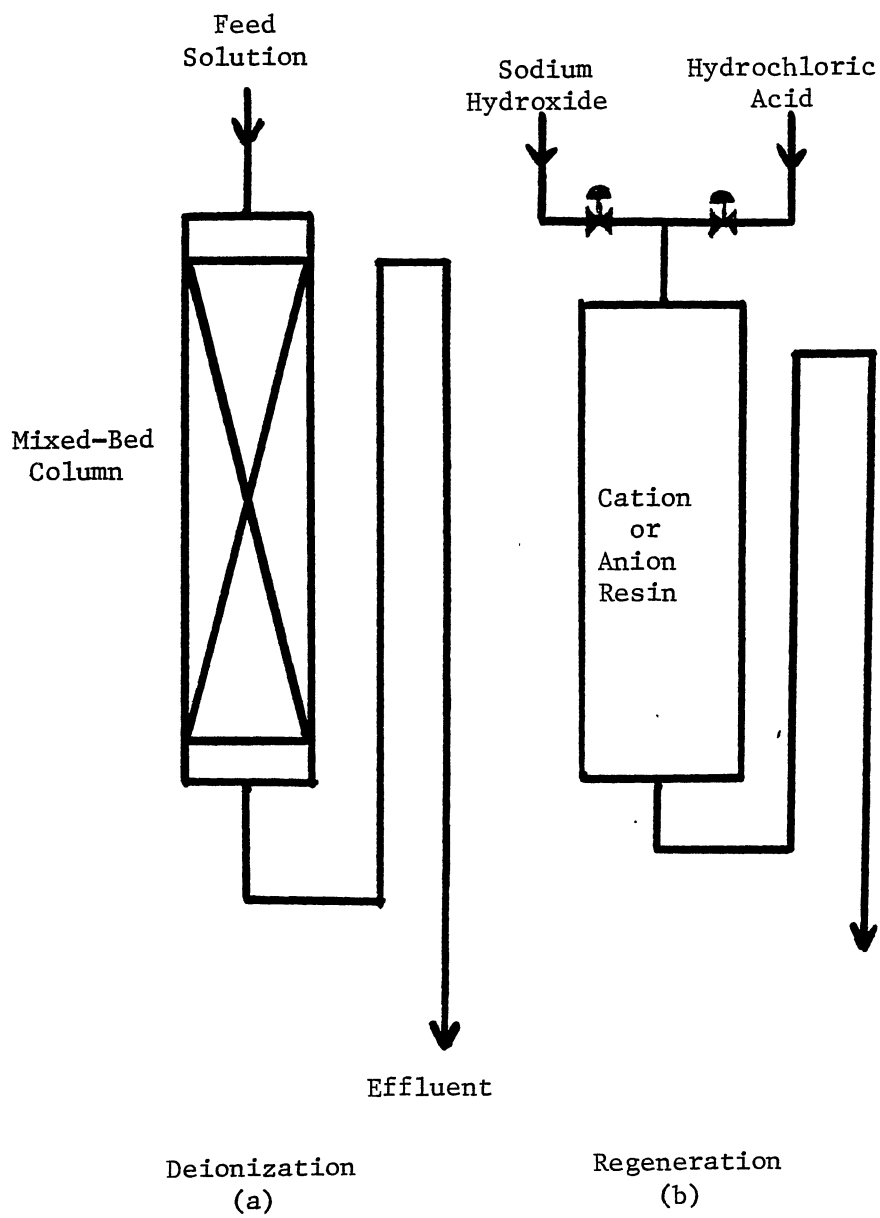


Figure 24. Experimental Set-up for Mixed-Bed Ion-Exchange Studies

3. The data on selectivity coefficients available today is rather scarce and incomplete. Extensive resin behavior studies can be conducted using the set-up described above. The resin selectivity coefficients can be correlated to their degrees of crosslinking, temperature and presence of other substances. Such detailed studies would help characterizing resins and directly illustrate their characteristics.

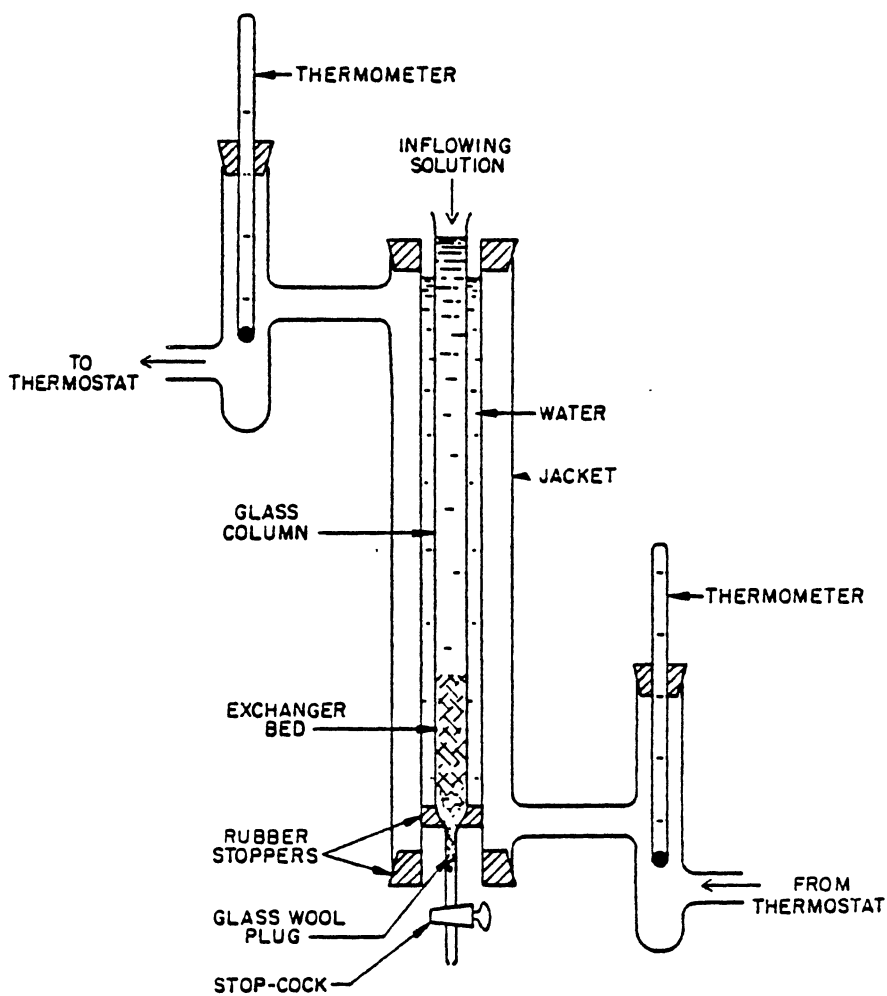


Figure 25. Jacketed Ion-Exchange Column (39)

BIBLIOGRAPHY

1. Adamson, A. W. and Grossman, J. J., J. Chem. Phys., 17, 1002 (1949).
2. Alfrey, T., Mechanical Behavior of High Polymers, Interscience Publishers Inc., New York, 1948.
3. Barrer, R. M., Klinowski, J., J. Chem. Soc. Faraday Trans. 1, 70(11), 2080-91 (1974).
4. Bonner, O. D., Pruett, R.R., J. Phys. Chem., 63(9), 1417 (1959).
5. Bonner, O. D., Smith, L. L., J. Phys. Chem., 1614, 61 (1957).
6. Boyd, G. E., Adamson, A. W., Myers, L. S., Jr., J Am. Chem. Soc., 69, 2836 (1947).
7. Boyd, G. E., Soldano, B. A., Z. Electrochem., 57, 162 (1953).
8. Boyd, G. E., Lindenbaum, S., Myers, G. E., J. Phys. Chem., 65, 577-86 (1961).
9. Braud, C., Selegny, E., Separ. Sci., 9(1) 13-19 and 21-26 (1974).
10. Carberry, J. J., A.I. Ch. E. J., 4, 460 (1960).
11. Darji, J. D., Proc. Am. Power. Conf. 42, 1101 (1980).
12. Dracheva, L. V., Rubinstein, R. N., Varshal, G. M., Ksenzenko, V. I., Zhur. Fiz. Khim., 50(2), 509-10 (1976).
13. Fabuss, B. M., Korosi, A., U.S. Office Saline Water Res. Develop. Progr. Rep., No. 249, 50 pp. (1967). Avail. G.P.O.
14. Flory, P. J., Principles of Polymer Chemistry, Chaps. X-XII, Cornell University Press, Ithaca, New York, 1953.
15. Freeman, D. H., J. Chem. Phys., 35, 189-91 (1961).
16. Gaines, G. L., Jr., Thomas, H. C., J. Chem. Phys., 21, 714 (1953).
17. Glueckauf, E., J. Soc. Chem. Ind. (London), 74, 34 (1955).
18. Glueckauf, E., Proc. Roy. Soc. (London), A214, 207 (1952).
19. Goldstein, S. and Murray, J. D., Proc. Roy Soc. (London), A252, 334, 348, 360 (1959).

20. Gregor, H. P., J. Am. Chem. Soc., 70, 1293 (1948); 73, 642 (1951).
21. Gregor, H. P., Belle, J., Marcus, R. A., J. Am. Chem. Soc., 77, 2713-19 (1955).
22. Guggenheim, E. A., Turgeon, J. C., Trans. Faraday Soc., 51, 747 (1955).
23. Harned, H. S., Robinson, R. A., Trans. Faraday Soc., 36 (1940) 973.
24. Harris, F. E., Rice, S. A., J. Chem. Phys., 24, 1258 (1956).
25. Haub, C. E. and Foutch, G. L., Mixed-Bed Ion Exchange at Concentrations Approaching the Dissociation of Water: 1. Water Development; 2. Column Model Applications, I. & E. C. Fund., 1986.
26. Helfferich, F. G. and Plesset, M. S., J. Chem. Phys., 28, 418 (1958).
27. Helfferich, F. G., Ion Exchange, McGraw Hill Book Company, New York, 1962.
28. Helfferich, F. G., in Ion Exchange, Vol. 1, J. Marinsky (ed.), p. 65, Marcel-Dekker Inc., New York, 1966.
29. Helfferich, F. G., J. Phys. Chem., 69, 1178 (1965).
30. Hiester, H. K. and Vermeulen, T., Chem. Eng. Prog., 48, 505 (1952).
31. Hines, A. L., Maddox, R. N., Mass Transfer, Prentice Hall Inc., New Jersey, 1985.
32. Holm, L. W., Arkiv Kemi (10) 151-166 (1956).
33. Kataoka, T. et al., J. Chem. Eng. Jap., 9, 74 (1976).
34. Kataoka, T. et al., J. Chem. Eng. Jap., 9, 130 (1976).
35. Kataoka, T. et al., J. Chem. Eng. Jap., 6, 172 (1973).
36. Kataoka, T. et al., J. Chem. Eng. Jap., 1, 38 (1968).
37. Katchalsky, A., Lifson, S., J. Polymer Sci., II, 409 (1953).
38. Katchalsky, A., Progr. Biophys., 4, 1 (1954).
39. Kielland, J. J., Soc. Chem. Ind. (London), 56, 232 T (1935).
40. Kitchener, J. A., Ion Exchange Resins, John Wiley & Sons Inc., New York, 1957.
41. Kraus, K. A., Raridon, R. J., J. Phys. Chem. 63, 1901, 1959.
42. Kraus, K. A., Raridon, R. J., Holcomb, D. L., J. Chromatog., 3, 178-179 (1960).

43. Krylova, A. A., Soldatov, V. S., Starobinets, G. L., Zhur. Fiz. Khim., 40(6) 1203-6 (1966) Russ.
44. Kuznetsova, E. M., Zhur. Fiz. Khim., 45 (10) 2581-3 (1971).
45. Lagos, A. E. and Kitchener, J. A., Trans. Faraday Soc., 56, 1245 (1960).
46. Lazare, L., Sundheim, B. R., Gregor, H. P., J. Phys. Chem., 60, 641 (1956).
47. Mackay, D., J. Phys. Chem. 64, 1718 (1960).
48. Makhija, R. C., Stairs, R. A., Can. J. Chem., 48, 1214 (1970).
49. Maron, S. H., Prutton, C. F., Principles of Physical Chemistry, Macmillan Co., New York, 1958.
50. Mears, P., Thain, J. F., J. Phys. Chem., 72(8) 2789-97 (1968).
51. Michaeli, I., Katchalsky, A., J. Polymer Sci., 23, 683 (1957).
52. Myers, G. E., Boyd, G. E., J. Phys. Chem., 60, 521 (1956).
53. Nelson, F., J. Polymer Sci., 40, 563 (1959).
54. Nernst, W., Z. Physik. Chem., 47, 52 (1904).
55. Pan, S. H. and David, M. M. (Paper presented at the A.C.S. national meeting, San Francisco, California, August, 1976), Seattle Washington: University of Washington, Dept. of Chemical Engineering, 1976.
56. Pasechnik, V. A., Samsonov, G. V., Elkin, G. E., Zhur. Fiz. Khim., 44(4) 1065-70 (1970).
57. Pauley, J. L., J. Am. Chem. Soc., 76, 1422 (1954).
58. Plasset, M. S., Helfferich, F. G., Franklin, J. N., J. Chem. Phys., 29, 1064 (1958).
59. Randin and Brunisholz, Helv. Chim. Acta., 46(6) 2107-10 (1963).
60. Reichenberg, D., and Wall, W. F., J. Chem. Soc., 3364 (1956).
61. Reid, R. C., Prausnitz, J. M., Sherwood, T. K., Properties of Gases and Liquids, McGraw-Hill Book Co., Third Edition, 1977.
62. Rice, S. A., Nagasawa, M., Polyelectrolyte Solutions, pp. 461-495, Academic Press, Inc., New York, 1961.
63. Robinson, R. A., Stokes, R. H., Electrolyte Solutions, p. 440, Butterworth's, London, 1955.

64. Ruvarac, A., Vesely, V., Z. Phys. Chem. (Frankfurt am Main), 73 (1-3), (1-6) Eng. (1970).
65. Schwarz, A., Boyd, G. E., J. Phys. Chem. 69(12) 4268-75 (1965).
66. Smith, T. G. and Dranoff, J. S., Ind. Eng. Chem. Fund., 3, 195 (1964).
67. Soldatov, V. S., Sokolova, V. I., Zhur. Fiz. Khim., 46(1), 146-8 (1972).
68. Soldatov, V. S., Starobinets, G. L., Zhur. Fiz. Khim., 38(3) 681-5 (1964).
69. Soldatov, V. S., Sokolova, V. I., Zhur. Fiz. Khim., 50(4), 943-5 (1976).
70. Thomas, H. C., J. Am. Chem. Soc., 66, 1664 (1944).
71. Tittle, K., Proc. Am. Power Conf., 43, 1126 (1981).
72. Tolmachev, A. M., Gorshkov, V. I., Zhur. Fiz. Khim., 49(8) 1924-29 (1966).
73. Van Brocklin, L. P. and David M. M., Ind. Eng. Chem. Fund., 11, 91 (1972).
74. Van Brocklin, L. P. and David, M. M., A. I. Ch. E. Symp. Ser., 71, 191 (1975).
75. Vermeulen, T., Advan. Chem. Eng., 2, 147 (1958).
76. Yurkova, L. S., Kolosva, A. F., Ol'shanova, K. M., Zhur. Fiz. Khim., 48(8), 2158 (1974).

2

VITA

Suhas Vasant Divekar

Candidate for the Degree of

Master of Science

Thesis: EFFECT OF TEMPERATURE ON MIXED-BED ION-EXCHANGE BASED ON LIQUID RESISTANCE CONTROLLED REACTIVE EXCHANGE MODEL AT LOW SOLUTION CONCENTRATIONS

Major Field: Chemical Engineering

Bibliographical:

Personal Data: Born in Gujarat, India, July 7, 1962, the son of Mr. and Mrs. V. Y. Divekar.

Education: Graduated from Don Basco Higher Secondary School, Madras, India in July, 1980; received Bachelor of Chemical Engineering degree from University of Bombay in July, 1984; completed requirements for Master of Science degree at Oklahoma State University in May, 1986.

Professional Experience: Trainee Engineer, Polychem Ltd., Bombay (India), May 1983 to July 1983; graduate teaching and research assistant, Oklahoma State University, School of Chemical Engineering, August 1984 to May 1986.